



Periocular Biometrics and its Relevance to Partially Masked Faces: A Survey

Renu Sharma^{a,**}, Arun Ross^a

^aDepartment of Computer Science and Engineering, Michigan State University, East Lansing, MI 48824, USA

ABSTRACT

The performance of face recognition systems can be negatively impacted in the presence of masks and other types of facial coverings that have become prevalent due to the COVID-19 pandemic. In such cases, the periocular region of the human face becomes an important biometric cue. In this article, we present a detailed review of periocular biometrics. We first examine the various face and periocular techniques specially designed to recognize humans wearing a face mask. Then, we review different aspects of periocular biometrics: (a) the anatomical cues present in the periocular region useful for recognition, (b) the various feature extraction and matching techniques developed, (c) recognition across different spectra, (d) fusion with other biometric modalities (face or iris), (e) recognition on mobile devices, (f) its usefulness in other applications, (g) periocular datasets, and (h) competitions organized for evaluating the efficacy of this biometric modality. Finally, we discuss various challenges and future directions in the field of periocular biometrics.

© 2022 Elsevier Ltd. All rights reserved.

1. Introduction

Biometrics is the automated or semi-automated recognition of individuals based on their physical (face, iris), behavioral (signature, gait), or psychophysiological (ECG, EEG) traits (Jain et al., 2011; Ross et al., 2019). The COVID-19 pandemic has ushered in a number of considerations for biometric systems. For example, in the context of fingerprint recognition, researchers are now investing more effort in designing contactless fingerprint systems (Yin et al., 2020; Lin and Kumar, 2019). Similarly, the prevalent use of face masks and social distancing protocols has refocused attention on occluded face recognition and, inevitably, ocular biometrics. The ocular region refers to the anatomical structures related to the eyes, and biometric cues in this region include pupil, iris, sclera, conjunctival vasculature, periocular region, retina, and oculomotor plant (comprising eye globe, muscles, and the neural control signals).

The term “periocular” has been used to refer to the region surrounding an eye consisting of eyelids, eyelashes, eye-folds, eyebrows, tear duct, inner and outer corner of an eye, eye shape, and skin texture (Figure 1). While many articles in the biometric literature include the sclera, iris, and pupil in the context of

periocular recognition (Park et al., 2009; Miller et al., 2010; De Marsico et al., 2017; Smereka and Kumar, 2017; Luz et al., 2018), others have excluded these regions (Woodard et al., 2010a,b; Park et al., 2011; Proena and Neves, 2018). The periocular region may be biocular (the periocular regions of both eyes are considered to be a single unit) (Jillela and Ross, 2012; Juefei-Xu and Savvides, 2012; Proena et al., 2014), monocular (either left or right periocular) (Park et al., 2009, 2011), or a fusion of the two monocular regions (combination of left and right periocular regions) (Bharadwaj et al., 2010; Woodard et al., 2010a; Boddeti et al., 2011). Earlier work (Park et al., 2009, 2011) on periocular biometrics studied its feasibility as a standalone biometric trait. Other researchers (Woodard et al., 2010b; Park et al., 2011; Juefei-Xu and Savvides, 2012) established its relevance by comparing it with the face and iris modalities. In some non-ideal conditions, the periocular region even shows higher performance than face (Miller et al., 2010; Park et al., 2011; Juefei-Xu and Savvides, 2012) and iris (Boddeti et al., 2011) modalities. Hollingsworth et al. ascertained its usefulness as a biometric trait by conducting human analysis on near-infrared (Hollingsworth et al., 2010; Hollingsworth et al., 2011; Hollingsworth et al., 2012) and visible (Hollingsworth et al., 2012) spectrum images.

Periocular recognition has numerous applications that go beyond the current pandemic (Figure 2). This includes (a) operat-

**Corresponding author:

e-mail: sharma90@cse.msu.edu (Renu Sharma)

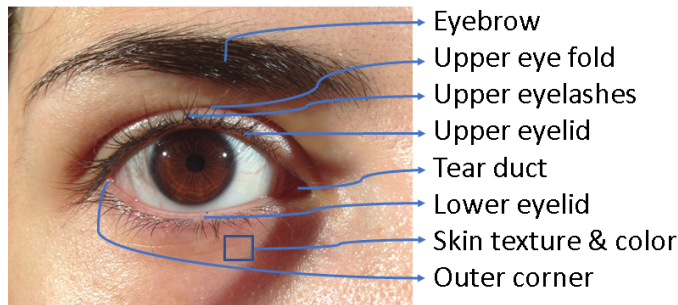


Fig. 1. Various components of the periocular region when viewed in the visible spectrum.

ing theaters where physicians wear surgical masks; (b) occupations where people wear helmets that occlude faces (e.g., military, astronauts, firefighters, bomb diffusion squads); (c) sporting events requiring a helmet (cricket, football, car racing); (d) use of veils to cover one's face due to cultural or religious purposes; and (e) robbers masking their faces to avoid being recognized. Periocular biometrics has various advantages, which further motivate its usage:

1. Periocular modality can be acquired using the sensors that capture face and iris modalities. So, there is typically no additional imaging requirement.
2. Compared to iris or other ocular traits (e.g., retina or conjunctival vasculature), periocular images can be captured in a relatively non-invasive, less constrained, and non-cooperative environment. They are also less prone to occlusions due to eyelids, eyeglasses, or deviated gaze. In contrast to the face modality, the periocular region (which is, of course, a part of the face) is relatively more stable as it is less affected by variations in pose, aging, expression, plastic surgery, and gender transformation. It is also seldom occluded when face images are captured in close quarters (e.g., selfies) or in the presence of scarves, masks, or helmets.
3. The periocular modality can complement the information provided by the iris and face modalities. So, it can be combined with the iris (Santos and Hoyle, 2012; Tan and Kumar, 2012; Raghavendra et al., 2013; Alonso-Fernandez and Bigun, 2015) and face (Jillela and Ross, 2012; Mahalingam et al., 2014) modalities to increase the performance of the biometric system without any modification to the acquisition setup.
4. It can also be used for other tasks such as presentation attack detection (Hoffman et al., 2019), and soft-biometrics extraction (Merkow et al., 2010; Lyle et al., 2012; Rattani et al., 2017; Alonso-Fernandez et al., 2018).
5. It can help with cross-spectral iris recognition (Santos et al., 2015) as iris images captured in different spectra depict different features, while periocular features (shape of the eye, eyelashes, eyebrows) are relatively stable. It also facilitates cross-modal (face-iris) matching (Jillela and Ross, 2014) as it is the common region present in both the modalities.

In the literature, there are previous surveys that focused on periocular biometrics (Santos and Proena, 2013; Nigam et al., 2015; Alonso-Fernandez and Bigun, 2016; Rattani and Derakhshani, 2017; Badejo et al., 2019; Behera et al., 2019; Kumari and Seeja, 2019). Santos and Proena (2013) summarized the significant papers on periocular recognition before 2013. The authors in (Nigam et al., 2015; Rattani and Derakhshani, 2017) discussed the research advances of various ocular biometric traits such as iris, periocular, retina, conjunctival vasculature and eye movement, and their fusion with other modalities. Alonso-Fernandez and Bigun (2016) described periocular recognition methodologies in terms of pre-processing, feature extraction, fusion, soft-biometric extraction, and other applications. Behera et al. (2019) focused on cross-spectral periocular recognition. Zanlorensi et al. (2021) provided detailed information on periocular and iris datasets, and competitions based on some of these datasets. A recent survey on periocular biometrics is in (Kumari and Seeja, 2019). Figure 3 shows a visualization of various research work on periocular biometrics. The main contributions of this paper lie in the detailed categorization of periocular techniques. We also describe periocular techniques specifically useful for human recognition in the COVID-19 pandemic.

In this paper, we present a comprehensive review of periocular biometrics. We discuss different categorizations based on (a) different anatomical cues utilized for recognition, (b) feature extraction or matching methodologies, (c) different spectral input images, and (d) fusion with different modalities. We then discuss periocular recognition techniques for mobile devices, in other applications (e.g., soft biometrics, iris presentation detection) and for recognition in special circumstances (cross-modal, gender transformation, long-distance). We also describe various periocular datasets and competitions held. Considering the COVID-19 pandemic situation, we also provide a brief review of recent face and periocular techniques specifically designed to recognize humans wearing a face mask.

The rest of the paper is organized as follows: Section 2 describes various face and periocular techniques specially applied on the masked faces for human identification, Section 3 categorizes periocular techniques based on anatomical cues utilize for recognition, Section 4 describes various periocular features extraction and matching techniques, Section 5 categorizes techniques based on input images of different spectra, Section 6 discusses fusion techniques with other biometric modalities, Section 7 provides details of periocular authentication on mobile devices, Section 8 describes periocular recognition in specific scenarios and other applications, Section 9 details periocular datasets and competitions, Section 10 focuses on various challenges and future directions, and Section 11 concludes the paper.

2. Periocular in COVID-19 Pandemic

Periocular recognition has gained relevance during the COVID-19 pandemic as some reports have documented a drop in performance of existing face recognition methods in the presence of facial masks (Damer et al., 2020; Ngan et al., 2020a,b).



Fig. 2. Various scenarios where the periocular region has increased significance: (a) girl with a mask during the covid pandemic, (b) doctors and nurses in the surgical room, (c) women in niqab, (d) partial faces in the crowd, (e) occluded face while drinking, (f) robber with face covering, (g) military personnel with face paint, (h) football player wearing a helmet, (i) cricket player wearing a helmet, (j) F1 race player in a helmet, (k) face-covering in cold weather, (l) astronauts in suit, (m) dancer with a face veil, (n) firefighter in uniform, and (o) people in motorbike helmets.

The tests conducted by NIST applied digitally tailored masks to face images for evaluation (6.2 million images from 1 million people). The first report (Ngan et al., 2020a) presented the performance of 89 algorithms that were submitted to NIST before the COVID-19 pandemic on the masked images. All 89 face recognition algorithms showed an increase in False Non-Match Rate (FNMR) by about 5% - 50% at a 0.001% False Match rate (FMR) - higher than NIST's prior study on unmasked images. The second report (Ngan et al., 2020b) published the performance of 65 new algorithms submitted to NIST after mid-March 2020 along with their previous submissions (cumulative results for 152 algorithms). The new algorithms include masked images during the enrollment stage. However, the report showed increased FNMR (5% - 40%) for all the newly submitted algorithms, though the new algorithms showed improved accuracy compared to the pre-pandemic algorithms. An earlier work by Park et al. (2011) also showed a drop in rank-one accuracy of a commercial face recognition software from 99.77% (full-face images) to 39.55% when the lower region was occluded.

In an era of masked faces necessitated by the pandemic, periocular information can be helpful for human recognition in two ways, either by generating a full face from the periocular region or by matching using only the periocular region. Juefei-Xu et al. (Juefei-Xu et al., 2014; Juefei-Xu and Savvides, 2016) hallucinated the entire face from the periocular region using dictionary learning algorithms. Ud Din et al. (2020) detected the masked region from a face image and then performed image completion on the masked region. They used a GAN-based network for image completion, which consists of two discriminators; one learns the global structure of the face and the other focuses on learning the missing region. Li et al. (2020) also performed face completion to recover the content under the mask through the de-occlusion distillation framework. Hoang et al. (2020) emphasized the use of eyebrows for human identification. Wang et al. (2020) released three datasets for face and periocular evaluation on masked images: Masked Face Detection Dataset (MFDD), Real-world Masked Face Recognition Dataset (RMFRD), and Simulated Masked Face Recognition Dataset (SMFRD). Anwar and Raychowdhury (2020) presented an open-source tool, MaskTheFace, to create masked faces images. Moreover, research work on face detection in the pres-

ence of masks (Opitz et al., 2016; Ge et al., 2017), face mask detection (Chowdary et al., 2020; Qin and Li, 2020; Loey et al., 2021) and face recognition under occlusion (Song et al., 2019; Ding et al., 2020; Geng et al., 2020; Boutros et al., 2021a; Damer et al., 2021; Hariri, 2021; Montero et al., 2021) would be helpful in human identification on masked face images. Various competitions are also conducted to benchmark face recognition techniques on masked faces (Deng et al., 2021; Boutros et al., 2021b; Zhu et al., 2021).

3. Anatomical Cues in the Periocular Region

Woodard et al. (2010b) classified periocular anatomical cues into two levels: level-one cues comprise eyelids, eye folds, eyelashes, eyebrows, and eye corners, while level-two includes skin texture, fine wrinkles, color, and skin pores. Specifically, level-one cues represent geometric nature of the periocular region, while level-two embodies textural and color attributes. The authors in (Hollingsworth et al., 2010; Hollingsworth et al., 2011; Park et al., 2011; Beom-Seok Oh et al., 2012) studied the significance of various periocular components in recognizing individuals. Earlier work on face recognition (Sadr et al., 2003) suggested the eyebrows to be the most salient and stable feature of the face. Hollingsworth et al. (Hollingsworth et al., 2010; Hollingsworth et al., 2011) conducted a human analysis to identify the discriminative cues on near-infrared (NIR) images and found that eyelashes, tear ducts, shape of the eye, and eyelids are the most frequently used cues in verifying the two images of a person. The studies in (Park et al., 2011; Beom-Seok Oh et al., 2012) utilized automatic feature descriptors to determine important regions on visible (VIS) spectrum images and concluded that eyebrows, iris, and sclera are the most significant cues for periocular performance. In a subsequent work (Hollingsworth et al., 2012), the authors applied both human and machine approaches to identify discriminative regions on both NIR as well as VIS periocular images. They observed that humans and computers both focus on the same periocular cues for identification: in VIS images, blood vessels, skin region, and eye shape are more salient, whereas in NIR images, eyelashes, tear ducts, and eye shape are more promising. Other authors (Smereka and Kumar, 2013; Alonso-Fernandez and Bigun, 2014; Smereka and Kumar, 2017) also drew similar con-

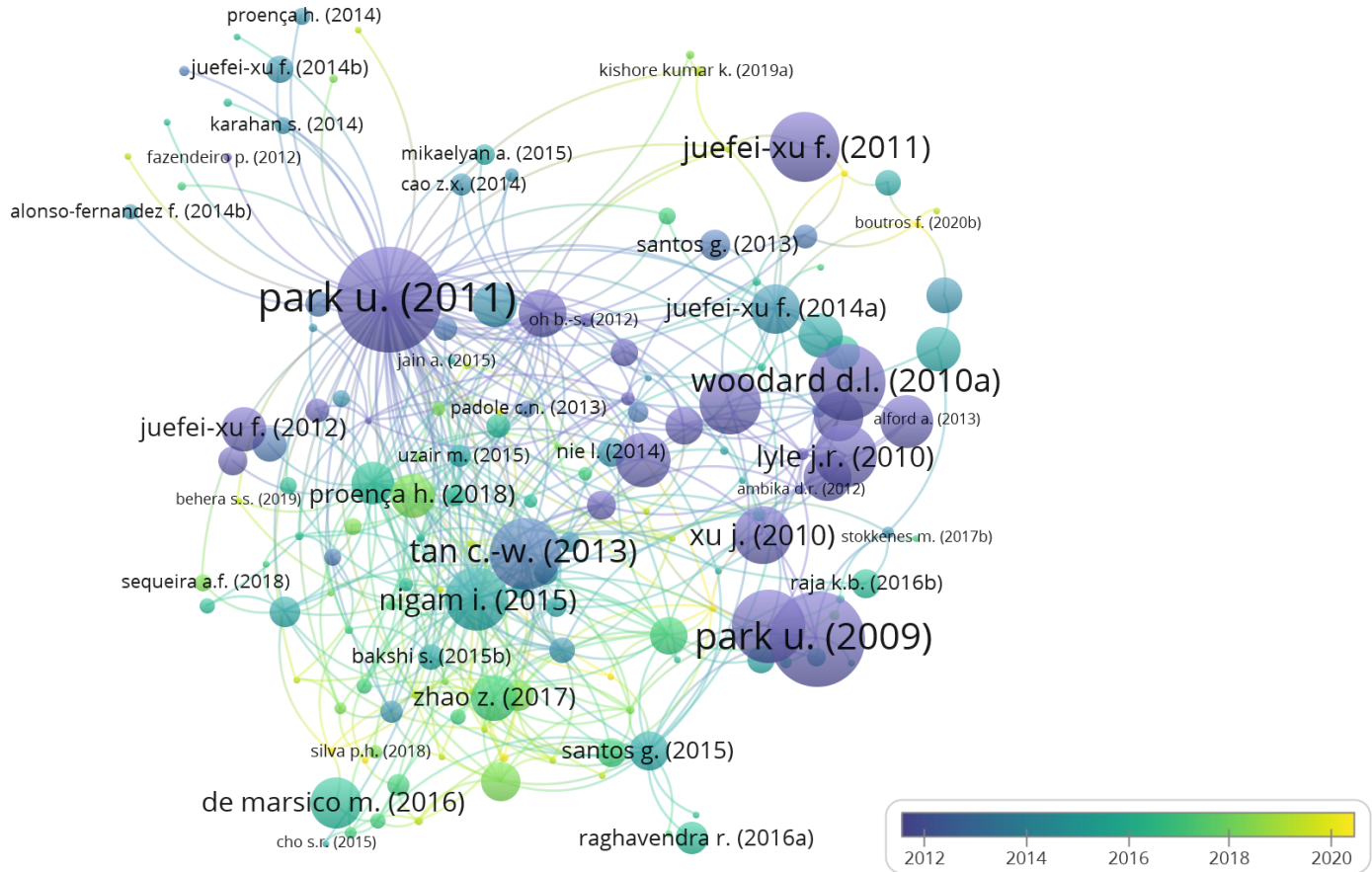


Fig. 3. Network visualization of research articles on periocular biometrics. The size of the node represents the number of citations, and its color represents the year of publication. Figure generated using VOSviewer software.

clusions on the relevance of periocular cues in VIS and NIR images. In summary, level-one cues are more useful for NIR images, whereas level-two cues aid in VIS images.

Researchers have also analyzed the utility of periocular cues as a standalone biometrics, for instance, using only the eyebrows (Dong and Woodard, 2011; Le et al., 2014; Hoang et al., 2020), or periocular skin (Miller et al., 2010), or eyelids (Proena, 2014). Details of the other ocular biometrics traits closely related to periocular can be found in the following studies: iris (Bowyer et al., 2008, 2013), sclera (Zhou et al., 2012; Das et al., 2013), conjunctiva vasculature (Derakhshani and Ross, 2007; Crihalmeanu and Ross, 2012), eye movements (Rigas et al., 2012; Holland and Komogortsev, 2013; Sun et al., 2014), oculomotor plant characteristics (Komogortsev et al., 2010), and gaze analysis (Cantoni et al., 2015). The description of these ocular traits is out of the scope of this paper.

4. Methodologies used for Periocular Recognition

A typical periocular recognition system consists of the following steps: acquisition, pre-processing of the acquired image, localization of region-of-interest (ROI), feature extraction, post-processing of extracted features, and matching of two feature sets. In the acquisition step, the periocular image is captured using a sensor or camera. We provide details of vari-

ous sensors used to capture periocular images along with their datasets in Section 9. The pre-processing step aims to enhance the visual quality of an image. Commonly, pre-processing techniques are applied to normalize illumination variations, such as anisotropic diffusion (Juefei-Xu and Savvides, 2012) and Multiscale Retinex (MSR) (Juefei-Xu et al., 2014; Nie et al., 2014). Karahan et al. (2014) applied histogram equalization for contrast enhancement. Juefei-Xu et al. (2011) performed pre-processing schemes for pose correction, illumination, and periocular region normalization. Proena and Briceo (2014) investigated an elastic graph matching (EGM) algorithm to handle nonlinear distortions in the periocular region due to facial expressions.

The localization step extracts the periocular region from the acquired or pre-processed image. As the definition of the periocular region has not yet been standardized, the ROI used for periocular recognition varies across the literature. The authors in (Tan and Kumar, 2012; Park et al., 2009; Mahalingam et al., 2014) considered the iris center as a reference point to determine the periocular rectangular region. The authors in (Padole and Proena, 2012; Nie et al., 2014) used the geometric mean of eye corners to localize the ROI since the iris center is affected by gaze, pose, and occlusion. Bakshi et al. (2013) localized the periocular region based on the anthropometry of the human face. Park et al. (2011) studied the effect of including

eyebrows in ROI on the recognition performance by performing both manual localization (based on the centers of the eyes) and automatic localization (based on the anthropometry of the human face). Algashaam et al. (2017b) analyzed the influence of varying periocular window sizes on periocular recognition performance. Kumari and Seeja (2021b) proposed an approach to extract optimum size periocular ROIs of two different shapes (polygon and rectangular) by using five reference points (inner and outer canthus points, two end points and the midpoint of eyebrow). Proena et al. (2014) described an integrated algorithm for labeling seven components of the periocular region in a single-shot: iris, sclera, eyelashes, eyebrows, hair, skin, and glasses. Deep learning techniques have also been used to detect the periocular region, such as ROI-based object detectors (Reddy et al., 2018b) and supervised semantic mask generators (Zhao and Kumar, 2018). Reddy et al. (2020) proposed spatial transformer network (STN), which is trained in conjunction with the feature extraction model to detect the ROI.

The feature extraction step involves the extraction of discriminative and robust features from the localized periocular region. Alonso-Fernandez and Bigun (2016) categorized feature extraction techniques into global and local approaches. We group deep learning-based approaches separately. Table 1 lists the various feature extraction techniques corresponding to these categories, along with research papers utilizing these techniques. The description of all three approaches are provided below.

1. Global Feature Approaches: The global feature extraction approaches consider the entire periocular ROI as a single unit and extract features based on texture, color, or shape. Texture in a digital image refers to the repeated spatial arrangement of the image pixels. Commonly used techniques to capture the textural features from the periocular region are Local Binary Patterns (LBP) and its variants (Park et al., 2009; Adams et al., 2010; Bharadwaj et al., 2010; Juefei-Xu et al., 2010; Miller et al., 2010; Xu et al., 2010; Juefei-Xu and Savvides, 2012; Beom-Seok Oh et al., 2012; Padole and Proena, 2012; Santos and Hoyle, 2012; Uzair et al., 2013; Cao and Schmid, 2014; Mahalingam et al., 2014; Nie et al., 2014; Sharma et al., 2014; Santos et al., 2015), Histogram of Oriented Gradients (HOG) (Park et al., 2009, 2011), Gabor filters (Juefei-Xu et al., 2010; Alonso-Fernandez and Bigun, 2012; Joshi et al., 2014; Cao and Schmid, 2014; Alonso-Fernandez and Bigun, 2015), and Binarized Statistical Image Features (BSIF) (Raghavendra et al., 2013; Raja et al., 2014a). The LBP descriptor computes the binary patterns around each pixel by comparing the pixel value with its neighborhood. The binary patterns are then quantized into histograms, which on concatenation form a feature vector. In the HOG descriptor, gradient orientation and magnitude around each pixel are binned into histograms and histograms are then concatenated to form a feature vector. The Gabor filters extract features by applying textural filters of different frequencies and orientations on an image. The BSIF descriptor convolves the image with a set of filters learned from natural images, and then the responses are binarized. Other texture-based features include Bayesian Graphical Models (BGM) (Boddeti et al., 2011), Probabilistic Deformation Models (PDM) (Ross

et al., 2012; Smereka and Kumar, 2013), Discrete Cosine Transform (DCT) (Juefei-Xu et al., 2010), Discrete Wavelet Transform (DWT) (Juefei-Xu et al., 2010; Joshi et al., 2014), Force Field Transform (FFT) (Juefei-Xu et al., 2010), GIST perceptual descriptors (Bharadwaj et al., 2010), Joint Dictionary-based Sparse Representation (JDSR) (Raghavendra et al., 2013; Jillela and Ross, 2014; Moreno et al., 2016), Laws masks (Juefei-Xu et al., 2010), Leung-Mallik filters (LMF) (Tan and Kumar, 2012), Laplacian of Gaussian (LoG) (Juefei-Xu et al., 2010), Correlation-based methods (Boddeti et al., 2011; Juefei-Xu and Savvides, 2012; Ross et al., 2012; Jillela and Ross, 2014), Phase Intensive Global Pattern (PIGP) (Smereka and Kumar, 2013; Bakshi et al., 2014), Structured Random Projections (SRP) (Oh et al., 2014), Walsh masks (Juefei-Xu et al., 2010), Higher Order Spectral (HOS) (Algashaam et al., 2017b), Gaussian Markov random field (Smereka et al., 2015), and Maximum Response (MR) (Raghavendra and Busch, 2016).

The color features of the periocular region correspond to the wavelengths of light reflected from its constituent parts. Woodard et al. (2010b) utilized the color features by applying histogram equalization on the luminance channel and then calculating the color histogram on the spatially salient patches of the image. Lyle et al. (2012) also extracted color features using local color histograms. Moreno et al. (2016) defined color components using linear and nonlinear color spaces such as red-green-blue (RGB), chromaticity-brightness (CB), and hue-saturation-value (HSV) and then applied a re-weighted elastic net (REN) model. The authors in (Woodard et al., 2010b; Moreno et al., 2016) utilized both textural and color features from the periocular recognition. Regarding shape features, the work in (Dong and Woodard, 2011; Le et al., 2014) utilized eyebrow shape-based features, while Proena (2014) extracted eyelid shape features. Ambika et al. (2016) employed LaplaceBeltrami operator to extract periocular shape characteristics. All aforementioned techniques use 2D image data of the periocular region. Chen and Ferryman (2015) combined 3D shape features extracted using the iterative closest point (ICP) method and fused them with 2D LBP textural features at the score-level. One of the major advantages of using global feature approaches is that they generate feature vectors of fixed-length, and matching of fixed-length vectors is computationally effective. However, global feature approaches are more susceptible to image variations, such as occlusions or geometric transformations.

2. Local Feature Approaches: The local feature extraction approaches first detect salient or key points from the ROI and then extract features from their local neighborhood to create a feature descriptor. Commonly used local feature approaches are Scale Invariant Feature Transformation (SIFT) (Xu et al., 2010; Park et al., 2011; Padole and Proena, 2012; Ross et al., 2012; Santos and Hoyle, 2012; Smereka and Kumar, 2013; Alonso-Fernandez and Bigun, 2014) and Speeded-up Robust Features (SURF) (Juefei-Xu et al., 2010; Xu et al., 2010; Raja et al., 2015b). The SIFT feature extractor defines key locations as extrema points on the difference of Gaussians (DoG) images obtained from a series of smoothed and rescaled images. Feature descriptor is then formed by concatenating orientation histograms defined around each key point. On the other hand,

SURF detects key points by utilizing the Hessian blob detector, and the key points are then described using Haar wavelet features. SURF utilizes integral images to speed up the computation. Other local feature descriptors are Binary Robust Invariant Scalable Keypoints (BRISK) (Mikaelyan et al., 2014), Oriented FAST and Rotated BRIEF (ORB) (Mikaelyan et al., 2014), Phase Intensive Local Pattern (PILP) (Bakshi et al., 2015), Symmetry Assessment by Feature Expansion (SAFE) (Mikaelyan et al., 2014; Alonso-Fernandez and Bigun, 2015), and Dense SIFT (Ahuja et al., 2016a). Since the number of detected key points varies among images, the resulting feature vectors also vary in length, making the process computationally expensive in some cases. However, local feature approaches are more robust to occlusions, illumination variations, and geometric transformations compared to global feature approaches.

3. Deep Learning Approaches: With the success of deep learning in computer vision and biometrics, this approach has also been applied to periocular recognition. Earlier work (Nie et al., 2014) based on learning approaches introduced an unsupervised convolutional version of Restricted Boltzmann Machines (CRBM) for periocular recognition. Raja et al. (Raja et al., 2016b, 2020) extracted features from Deep Sparse Filters using transfer learning methodology and input them into a dictionary-based approach for classification. On the other hand, Raghavendra and Busch (2016) extracted texture features using Maximum Response (MR) filters and input them into deep coupled autoencoders for classification. Other studies that utilized transfer learning methodologies can be found in (Luz et al., 2018; Silva et al., 2018; Kumari and Seeja, 2020). Proena and Neves (2018) utilized deep CNN to emphasize the importance of the periocular region for recognition by training the network with augmented periocular images having inconsistent iris and sclera regions. The training procedure causes the network to implicitly disregard the iris and sclera region. The authors in (Zhao and Kumar, 2018; Wang and Kumar, 2021) integrated attention model to the deep architecture in order to highlight the significant regions (eyebrow and eye) of the periocular image. Some researchers utilized existing off-the-shelf CNN models to extract deep features at various convolutional levels (Hernandez-Diaz et al., 2018; Kim et al., 2018; Hwang and Lee, 2020; Kumari and Seeja, 2020, 2021a). The authors in (Zhang et al., 2018; Reddy et al., 2018a) proposed compact and custom deep learning models for use in mobile devices. Other deep learning-based methods include PatchCNN (Reddy et al., 2018b), In-Set CNN Iterative Analysis (Proena and Neves, 2019), unsupervised convolutional autoencoders (Reddy et al., 2019), compact Convolutional Neural Network (CNN) (Reddy et al., 2020), VisobNet (Ahuja et al., 2017), semantics assisted CNN (Zhao and Kumar, 2017), heterogeneity aware deep embedding (Garg et al., 2018), and Generalized Label Smoothing Regularization (GLSR)-trained networks (Jung et al., 2020). Deep learning approaches provide state-of-the-art recognition performance, but their performance are heavily data-driven.

After the feature extraction step, some researchers further processed the feature vector, which generally includes the application of feature selection, subspace projection, or dimen-

sional reduction (Beom-Seok Oh et al., 2012; Joshi et al., 2014) techniques. These techniques aim to transform the feature set into a condensed representative feature set such that it improves the accuracy and reduces the computational complexity. Various post-processing techniques used in periocular recognition are Principal Component Analysis (PCA) (Beom-Seok Oh et al., 2012), Direct Linear Discriminant Analysis (DLDA) (Joshi et al., 2014), and Particle Swarm Optimization (Silva et al., 2018). Finally, the processed features are compared using similarity or dissimilarity metrics such as Bhattacharya distance (Woodard et al., 2010a), Hamming distance (Oh et al., 2014), I-Divergence metric (Cao and Schmid, 2014), Euclidean distance (Ambika et al., 2016), or Mahalanobis distance (Nie et al., 2014).

5. Periocular Recognition in Different Spectra

Different imaging spectra have been described in the literature for capturing the periocular region, including Near-Infrared (NIR), Visible (VIS), Short Wave Infrared (SWIR), Middle Wave Infrared (MWIR), and Long Wave Infrared (LWIR). The most commonly used imaging spectra are NIR and VIS. This is because most research in periocular biometrics is based on face images (VIS) or iris images (NIR). Further, even as a standalone biometric, periocular images are captured using existing face or iris sensors. The NIR spectrum, which operates in the 700-900nm range, predominantly captures the iris pattern, eye shape, outer and inner corner of the eye, eyelashes, eyebrows, and eyelids. Often there is saturation in the area around the eye, skin, and cheek regions. On the other hand, the VIS spectrum (400-700nm) captures textural details of the periocular skin region, conjunctiva vasculature, eye shape, eyelashes, eyebrows, and eyelids. The VIS imaging fails to capture the textural nuances of the iris pattern, especially for dark-colored irides. Examples of periocular recognition techniques in the NIR spectrum are (Monwar et al., 2013; Uzair et al., 2013; Hwang and Lee, 2020; Mikaelyan et al., 2014), and in the VIS spectrum are (Adams et al., 2010; Bharadwaj et al., 2010; Park et al., 2009; Juefei-Xu et al., 2010; Miller et al., 2010; Woodard et al., 2010b; Xu et al., 2010; Park et al., 2011; Beom-Seok Oh et al., 2012; Padole and Proena, 2012; Santos and Hoyle, 2012; Joshi et al., 2014; Nie et al., 2014; Proena and Briceo, 2014; Proena et al., 2014; Bakshi et al., 2015; Santos et al., 2015; Hernandez-Diaz et al., 2018; Luz et al., 2018; Reddy et al., 2019). Rattani and Derakhshani (2017) provided a detailed survey of ocular techniques in the VIS spectrum. The researchers in (Hollingsworth et al., 2010; Smereka and Kumar, 2017) suggested that VIS images provide more discriminative information for periocular recognition compared to NIR images. Hollingsworth et al. (2012) made the same conclusion using human volunteers. The authors in (Alonso-Fernandez and Bigun, 2012; Ross et al., 2012; Alonso-Fernandez and Bigun, 2015; Smereka et al., 2015; Ambika et al., 2016; Zhao and Kumar, 2017) proposed periocular recognition techniques that can be applied to both NIR and VIS images. Other researchers (Al-gashaam et al., 2017a; Vetrekar et al., 2018; Ipe and Thomas, 2020) fused information obtained from both NIR and VIS images. Table 2 provides a summary (features extraction, datasets,

Table 1. A list of feature extraction techniques under global, local, and deep learning categories, along with some representative research papers describing these techniques.

Features	References	Features	References
Global Features			
Local Binary Patterns (LBP)	(Park et al., 2009; Bharadwaj et al., 2010; Xu et al., 2010; Beom-Seok Oh et al., 2012) (Padole and Proena, 2012; Santos and Hoyle, 2012; Uzair et al., 2013) (Mahalingam et al., 2014; Nie et al., 2014; Sharma et al., 2014; Bakshi et al., 2015) (Juefei-Xu et al., 2010; Miller et al., 2010; Santos et al., 2015) (Juefei-Xu and Savvides, 2012; Cao and Schmid, 2014)	Bayesian Graphical Models (BGM)	(Boddeti et al., 2011)
Gabor filters	(Juefei-Xu et al., 2010; Alonso-Fernandez and Bigun, 2012) (Cao and Schmid, 2014; Joshi et al., 2014) (Alonso-Fernandez and Bigun, 2015)	Force Field Transform (FFT)	(Juefei-Xu et al., 2010)
Probabilistic Deformation Models (PDM)	(Ross et al., 2012; Smereka and Kumar, 2013)	GIST perceptual descriptors	(Bharadwaj et al., 2010)
Binarized Statistical Image Features (BSIF)	(Raghavendra et al., 2013; Raja et al., 2014a)	Leung-Mallik filters (LMF)	(Tan and Kumar, 2012)
Joint Dictionary-based Sparse Representation	(Raghavendra et al., 2013; Jillela and Ross, 2014; Moreno et al., 2016)	Laplacian of Gaussian (LoG)	(Juefei-Xu et al., 2010)
Discrete Wavelet Transform (DWT)	(Juefei-Xu et al., 2010; Joshi et al., 2014)	Laws masks	(Juefei-Xu et al., 2010)
Histogram of Oriented Gradients (HOG)	(Park et al., 2009, 2011; Algashaam et al., 2017b)	Discrete Cosine Transform (DCT)	(Juefei-Xu et al., 2010)
Phase Intensive Global Pattern (PIGP)	(Smereka and Kumar, 2013; Bakshi et al., 2015)	Normalized Gradient Correlation (NGC)	(Jillela and Ross, 2014)
Structured Random Projections (SRP)	(Oh et al., 2014)	Walsh masks	(Juefei-Xu et al., 2010)
Shape-based features	(Dong and Woodard, 2011; Proena, 2014) (Le et al., 2014; Ambika et al., 2016)	Gaussian Markov random field	(Smereka et al., 2015)
Maximum Response (MR)	(Raghavendra and Busch, 2016)	2D and 3D features	(Chen and Ferryman, 2015)
Color-based features	(Woodard et al., 2010a; Lyle et al., 2012; Moreno et al., 2016)	Genetic and Evolutionary Feature Extraction	(Adams et al., 2010)
Local Features			
Scale Invariant Feature Transformation (SIFT)	(Xu et al., 2010; Park et al., 2011; Padole and Proena, 2012) (Ross et al., 2012; Santos and Hoyle, 2012; Smereka and Kumar, 2013) (Alonso-Fernandez and Bigun, 2014; Ahuja et al., 2016a)	Binary Robust Invariant Scalable Key points (BRISK)	(Mikaelyan et al., 2014)
Speeded-up Robust Features (SURF)	(Juefei-Xu et al., 2010; Xu et al., 2010) (Bakshi et al., 2015; Raja et al., 2015b)	Phase Intensive Local Pattern (PILP)	(Bakshi et al., 2015)
Symmetry Assessment by Feature Expansion (SAFE)	(Mikaelyan et al., 2014; Alonso-Fernandez and Bigun, 2015)	Oriented FAST and Rotated BRIEF (ORB)	(Mikaelyan et al., 2014)
Deep Learning Techniques			
Off-the-shelf CNN Features	(Hernandez-Diaz et al., 2018; Kim et al., 2018) (Hwang and Lee, 2020; Kumari and Seeja, 2021a) (Ahuja et al., 2017; Luz et al., 2018) (Silva et al., 2018; Kumari and Seeja, 2020)	Convolutional Restricted Boltzman Machines (CRBM)	(Nie et al., 2014)
Transfer Learning	(Raja et al., 2016b, 2020)	PatchCNN	(Reddy et al., 2018b)
Deep Sparse Filters	(Raja et al., 2016b, 2020)	In-Set CNN Iterative Analysis	(Proena and Neves, 2019)
Custom and Compact CNNs	(Reddy et al., 2018a; Zhang et al., 2018; Reddy et al., 2020)	Semantics Assisted CNN	(Zhao and Kumar, 2017)
Autoencoders	(Raghavendra and Busch, 2016; Reddy et al., 2019)	Heterogeneity Aware Deep Embedding	(Garg et al., 2018)
Attention Models	(Zhao and Kumar, 2018; Wang and Kumar, 2021)	Generalized Label Smoothing Regularization (GLSR)	(Jung et al., 2020)

and performance) of various techniques applied on NIR, VIS, both spectrum, and multi-spectral (fusion of NIR and VIS) images.

A vast amount of research has also focused on cross-spectrum matching, where enrolled images are in one spectrum, while probe images are in another spectrum. The cross-spectrum evaluation scenario implicitly encapsulates the cross-sensor scenario (enrolled and probes images are from different sensors) as well. Examples of papers discussing the cross-spectrum scenario are (Cao and Schmid, 2014; Sharma et al., 2014; Ramaiah and Kumar, 2016; Behera et al., 2017; Raja et al., 2017; Hernandez-Diaz et al., 2019; Alonso-Fernandez et al., 2020; Behera et al., 2020; Hernandez-Diaz et al., 2020; Zanolensi et al., 2020; Vyas, 2022). Behera et al. (2019) provided a detailed survey on cross-spectrum periocular recognition. A more difficult evaluation scenario is when testing is performed on different datasets (cross-dataset) as it has to account for the variations due to different sensors, data acquisition environments, and subject population. Examples of cross-dataset evaluation can be found in (Reddy et al., 2019, 2020). Table 3 summarizes various cross-spectrum and cross-dataset techniques. The cross-sensor techniques are mainly evaluated on different mobile devices, so we provide these details in Section 7 (Periocular Recognition on Mobile Devices).

6. Periocular Fusion with Other Modalities

Simultaneous acquisition of periocular with the iris modality, and its complementary nature with respect to iris, has motivated

researchers to fuse periocular with iris to improve the overall recognition performance. The authors in (Woodard et al., 2010a; Ross et al., 2012) proposed the fusion of periocular with iris to improve the performance when acquired iris images are of low quality due to partial occlusions, specular reflections, off-axis gaze, motion and spatial blur, non-linear deformations, contrast variations, and illumination artifacts. The fusion is also helpful when iris images are captured from a distance as the periocular region is relatively stable even at a distance (Tan and Kumar, 2012). It is also advantageous when iris images are acquired in the visible spectrum (Santos and Hoyle, 2012; Tan and Kumar, 2013; Proena, 2014; Jain et al., 2015; Silva et al., 2018), or using mobile devices (Santos et al., 2015; Ahuja et al., 2016b). The iris texture is better discernible in NIR illumination, whereas periocular features become more perceptible in VIS illumination (Alonso-Fernandez and Bigun, 2015; Alonso-Fernandez et al., 2015). The overall performance obtained on the fusion of iris and periocular traits is generally better than using the iris only as shown in (Komogortsev et al., 2012; Raghavendra et al., 2013; Raja et al., 2014a; Ahmed et al., 2017; Verma et al., 2016). The fusion of iris and periocular is mainly performed at the score-level (Woodard et al., 2010a; Tan et al., 2012; Tan and Kumar, 2012; Raghavendra et al., 2013; Tan and Kumar, 2013; Proena, 2014; Alonso-Fernandez et al., 2015; Jain et al., 2015; Santos et al., 2015; Verma et al., 2016; Ahuja et al., 2016b; Algashaam et al., 2021), though there is some work on feature-level (Jain et al., 2015; Stokkenes et al., 2017; Silva et al., 2018) and decision-level (Santos and Hoyle, 2012) fusion also. Ogawa and Kameyama (2021) proposed Multi Modal Selector that adaptively selects a iris and periocu-

Table 2. A chronological overview (description, datasets, and performance) of periocular techniques utilizing NIR, VIS, or multispectral images. Here, RR is Recognition Rate, EER is Equal Error Rate, TMR is True Match Rate, FRR is False Rejection Rate, and FAR is False Acceptance Rate. The acronyms used in the ‘Description’ column are defined in the text or in the referenced papers.

Paper	Description	Datasets and Performance
NIR Spectrum		
(Uzair et al., 2013)	Formulate as an image set classification problem, where each image set corresponds to single subject	MBGC: RR is 97.70%
(Monwar et al., 2013)	PDM, modified SIFT, GOH features Fusion: Highest rank, borda count, plurality voting, markov chain rule at rank-level	FOCS: RR is 99.2%
(Mikaelyan et al., 2014)	Symmetry patterns	BioSec: EER is 10.75%
(Hwang and Lee, 2020)	Mid-level CNN features (plain CNN, ResNet, deep plane CNN, and deep ResNet) + Features selection	Proprietary: EER is 11.51% CASIA-Iris-Lamp: EER is 0.64%
Visible Spectrum		
(Park et al., 2009)	HOG, LBP, SIFT	FRGC: RR is 79.49%(SIFT)
(Xu et al., 2010)	Comparison of different features and their fusion	FRGC: TMR of 61.2% 0.1% FMR
(Adams et al., 2010)	GEFE+LBP	FRGC: RR is 92.16% FERET: RR is 85.06%
(Juefei-Xu et al., 2010)	LBP, WLBP, SIFT, DCT, Gabor filters, Walsh masks, DWT, SURF Law Masks, Force Fields, LoG	FRGC: RR is 53.2%(LBP+DWT) FG-NET: RR is 53.1%(LBP+DCT)
(Park et al., 2011)	Fusion of HOF, LBP and SIFT	FRGC: RR is 87.32%
(Padole and Proena, 2012)	HOG, LBP, SIFT	UBIPr: EER is ~20%(HOG + LBP + SIFT)
(Santos and Hoyle, 2012)	LBP, SIFT	UBIRIS v2: EER is 31.87% and RR is 56.4%
(Joshi et al., 2014)	Gabor-PPNN, DWT, LBP, HOG	MBGC: EER is 6.4%, GTDB: EER is 5.9%, IITK: EER is 15.5%, PUT: EER is 4.8%
(Nie et al., 2014)	PCA to: CRBM, SIFT, LBP, HOG	UBIPr: EER is 6.4% and RR is 50.1%
(Proena and Briceo, 2014)	GC-EGM to: LBP + HOG + SIFT	FaceExpressUBI: EER is 16%
(Hernandez-Diaz et al., 2018)	Fusion of off-the-shelf CNN (AlexNet, GoogLeNet, ResNet, and VGG) features and traditional features	UBIPr: EER of 5.1% and FRR is 11.3% at 1% FAR
(Jung et al., 2020)	Generalized label smoothing regularization-trained networks	ETHNIC, PUBFIG, FACESCUB, AND IMDB WIKI: avg.RR is 88.7% and EER of 10.4%
NIR and VIS Spectrum		
(Woodard et al., 2010b)	Tessellated image + Histograms of texture and color	FRGC (VIS): RR is 91%, MBGC (NIR): RR is 87%
(Ross et al., 2012)	Fusion of GOH, PDM, SIFT features at the score-level	FOCS (NIR): EER is 18.8%, FRGC (VIS): EER is 1.59%
(Alonso-Fernandez and Bigun, 2015)	Gabor features	4 NIR datasets: Accuracy is 97% 2 VIS datasets: Accuracy is 27%
(Bakshi et al., 2015)	Raw pixels, LBP, PCA, LBP + PCA	MGBC: NIR- RR is 99.8%, VIS- RR is 98.5% CMU Hyperspectral: RR is 97.2%, UBIPr: RR is 99.5%
(Ambika et al., 2016)	LaplaceBeltrami based shape features	CASIA FV1: accuracy is 95%, Basel 3D: Accuracy is 97% 3D periocular: Accuracy is 97.5%
(Smereka et al., 2015)	Periocular probabilistic deformation models	2 NIR and 3 VIS images datasets
(Zhao and Kumar, 2017)	Semantics-assisted convolutional neural networks	UBIRIS.V2: RR is 82.43%, FRGC: RR is 91.13%, FOCS: RR is 96.93%, CASIA.v4-distance: RR is 98.90%
Multi-spectrum		
(Algashaam et al., 2017a)	Multimodal compact multi-linear pooling feature fusion	IMP: Accuracy is 91.8%
(Vetrekar et al., 2018)	HOG, GIST, Log-Gabor transform and BSIF + CRC	Proprietary: RR is 96.92%
(Ipe and Thomas, 2020)	Fusion of the off-the-shelf CNN feature	IMP: Accuracy is 97.14%

Table 3. A chronological overview (description, datasets, and performance) of periocular techniques working under cross-spectrum and cross-dataset scenarios. Here, GAR is Genuine Acceptance Rate, GMR is Genuine Match Rate, FMR is False Match Rate, and d' is the separation between the mean of genuine and impostor distributions. The acronyms used in the ‘Description’ column are defined in the text or in the referenced papers.

Paper	Description	Datasets and Performance	
		Cross-spectrum	
(Cao and Schmid, 2014)	Gabor LBP, Generalized LBP, Gabor Weber descriptors	Pre-Tinders, TINDERS, PCSO (GAR at 0.1 FAR): SWIR-VIS: 0.75, NIR-VIS: 0.35, MWIR-VIS: 0.35	
(Sharma et al., 2014)	Combined neural network architecture	IMP (GAR @ 1% FAR): VIS-NV: 71.93%, VIS-NIR: 47.08%, NV-NIR: 48.21%	
(Ramaiah and Kumar, 2016)	Three patch LBP + MRF	(GAR @ 0.1% FAR) IMP (NIR-VIS): 18.35%, PolyU (NIR-VIS): 73.2%	
(Raja et al., 2017)	Steerable pyramids + SVM + Fusion of different scales	CROSS-EYED2016 (NIR-VIS): GMR is 100% at 0.01% FMR	
(Behera et al., 2017)	Difference of Gaussian + HOG + Cosine similarity	IMP (NIR-VIS): GAR is 25.03% at 0.1 FAR, EER is 45.29% PolyU: GAR is 83.12% at 0.1 FAR, EER is 13.87% CROSS-EYED2016: GAR is 89.27% at 0.1 FAR and EER is 13.22%	
(Hernandez-Diaz et al., 2019)	ResNet101 features + Chi-square distance, Cosine similitude	IMP (EER, GAR at 1% FAR): VIS-NV: (5.13%, 88.19) VIS-NIR: (5.19%, 88.13); NIR-NV: (10.19%, 81.55)	
(Hernandez-Diaz et al., 2020)	Convert NIR and VIS images using cGAN + CNN features	PolyU (NIR-VIS): EER is 1%, GAR is 99.1% at FAR=1%	
(Zanlorensi et al., 2020)	Fine-tune CNN models (VGG16, ResNet-50)	PolyU (NIR-VIS): EER is 0.35% and d is 7.75	
(Behera et al., 2020)	Variance-guided attention-based twin deep network	PolyU: EER is 6.38%, GAR is 96.17% at 10% FAR CROSS-EYED2016: EER is 2.36%, and GAR is 99.70% at 10% FAR IMP (EER, GAR at 10%FAR): VIS-NV: (9.71%, 90.62%) VIS-NIR: (13.59%, 82.49%), NIR-NV: (7.06%, 95.17%)	
(Alonso-Fernandez et al., 2020)	Fuse HOG, LBP, SIFT, Symmetry Descriptors, Gabor, Steerable Pyramidal Phase, VGG-Face, Resnet101, and Densenet201 features using LLR at score-level	CROSS-EYED2016: EER is 0.2%, FRR is 0.47% at 0.01% FAR VSSIRIS: EER is 0.2%, FRR 0.3% at 0.01% FAR	
Cross-datasets			
(Reddy et al., 2019)	Unsupervised convolutional autoencoders	Train: UBIRIS-V2, UBIPr, MICHE; Test: VISOB: EER is 12.23%	
(Reddy et al., 2020)	CNN features	Train: VISOB, Test: UBIRIS-V2: EER is 7.65%, UBIPr: EER is 3.87% CROSS-EYED2016: EER is 0.94%, CASIA-TWINS: EER is 9.41% FERET: EER is 0.06%	

lar classifier useful for human recognition.

The fusion of periocular with the face modality is also a viable option as periocular is a part of the face, and no additional acquisition is required. Though the periocular region is already accounted in face recognition as a part of the face, isolating the periocular and performing region-specic feature extraction provides an overall improvement in recognition performance. The fusion of face with periocular is also beneficial when face images are occluded, having large pose variations, or captured at a very close distance (e.g., a selfie). The work of periocular fusion with face in the context of plastic surgery (Jillela and Ross, 2012), gender transformation (Mahalingam et al., 2014) and mobile devices (Raja et al., 2015a; Pereira and Marcel, 2015) shows improved recognition accuracy. Table 4 summarizes various techniques that fuse periocular with iris and face modalities. In another research work, Oh et al. (2014) fused periocular features (structured random projections) with binary sclera features at the score-level for identity verification. Nigam et al. (2015) provided a detailed survey on the fusion of various ocular biometrics.

7. Periocular Recognition on Mobile Devices

The extensive usage of mobile devices motivates the need for human authentication on mobile devices for various purposes, such as access control, digital payments, or mobile banking. Several mobile devices are now emerging with integrated biometric sensors – iPhone 12 has a Touch ID fingerprint sensor and Face ID cameras, and the Samsung Galaxy S20 series has an in-display fingerprint sensor and an iris scanner. Periocular images are generally acquired using the front or rear camera of mobile devices in the visible spectrum. The challenges in mobile biometrics are low-quality input images and relatively limited computational power. The low-quality images are due

to hardware limitations and less constrained capturing environments. Raja et al. (2014b) explored periocular recognition on smart devices using well known feature extraction techniques (SIFT, SURF, and BSIF) and achieved a Genuine Match Rate (GMR) of 89.38% at 0.01% False Match Rate (FMR). There is some work on NIR images captured from mobile devices (Bakshi et al., 2018; Zhang et al., 2018). Bakshi et al. (2018) utilized a reduced version of Phase Intensive Local Pattern (PILP) features, whereas (Zhang et al., 2018) fused compact CNN features of iris and periocular through a weighted concatenation. Majority of the periocular-based mobile biometrics are performed on VIS images (Pereira and Marcel, 2015; Raja et al., 2015b; Ahuja et al., 2016a; Keshari et al., 2016; Raja et al., 2016b; Raghavendra and Busch, 2016; Ahmed et al., 2017; Ahuja et al., 2017; Rattani and Derakhshani, 2017; Stokkenes et al., 2017; Boutros et al., 2020; Krishnan et al., 2020; Raja et al., 2020). Keshari et al. (2016) investigated periocular recognition on pre- and post-cataract surgery mobile images. Krishnan et al. (2020) investigated the fairness of mobile ocular biometrics methods across gender. The work in (Pereira and Marcel, 2015; Raja et al., 2015b; Ahmed et al., 2017; Zhang et al., 2018) used fusion of different modalities for mobile biometrics – Raja et al. (2015b) fused iris, face and periocular modalities, (Pereira and Marcel, 2015) combined face and periocular, whereas (Santos et al., 2015; Ahmed et al., 2017; Zhang et al., 2018) combined iris and periocular. Recent work on mobile biometrics used deep learning features (Raja et al., 2016b; Raghavendra and Busch, 2016; Ahuja et al., 2017; Rattani and Derakhshani, 2017; Raja et al., 2020). Boutros et al. (2020) verified an individual wearing Head Mounted Display (HMD) using four handcrafted feature extraction methods and two deep-learning strategies. Generalizability across different mobile sensors (cross-sensor) are also evaluated in (Santos et al., 2015; Raja et al., 2016a,c; Garg et al., 2018; Reddy et al., 2018b;

Table 4. A chronological overview (description, datasets, and performance) of periocular techniques focusing on the fusion of periocular with iris and face modalities. Here, AUC is Area Under the Curve. The acronyms used in the ‘Description’ column are defined in the text or in the referenced papers.

Paper	Description	Datasets and Performance
Fusion of Iris and Periocular		
(Woodard et al., 2010a)	Iris: Gabor features, Periocular: LBP Fusion: Weighted sum at score-level	MBGC: EER is 0.18, RR is 96.5%
(Santos and Hoyle, 2012)	Iris: Wavelets, Periocular: LBP, SIFT Fusion: Logistic regression at decision-level	NICE.II: EER is 18.48, AUC is 0.90, RR is 74.3%
(Tan et al., 2012)	Iris: Ordinal measures and color analysis Periocular: Texton representation and semantic information Fusion: Weighted sum rule at score-level	USIRISv2: d is 2.57, EER is 12%
(Tan and Kumar, 2012)	Iris: Log-Gabor features Periocular: SIFT, Leung-Malik filters, LBP Fusion: Weighted sum rule at score-level	CASIA-IrisV4-distance: RR is 84.5%
(Tan and Kumar, 2013)	Iris: Log-Gabor features Periocular: DSIFT, GIST, LBP, HOG, LMF Fusion: Weighted sum rule at score-level	UBIRIS V2: RR is 39.6% FRGC: RR is 59.9% CASIA-IrisV4-Distance: RR is 93.9%
(Raghavendra et al., 2013)	Iris, Periocular: LBP-SRC, Fusion: Weighted sum at score-level	Proprietary: EER is 0.81%
(Proena, 2014)	Iris: Multi-lobe differential filters Eyelids, Eyelashes, Skin: shape and LBP features Fusion: Product, sum, min and max rule at score-level	UBIRISv2: d is 2.97 and AUC is 0.96 FRGC: d is 3.02 and AUC is 0.97
(Santos et al., 2015)	Iris: Gabor features, Periocular: SIFT, GIST, LBP, HOG, ULBP Fusion: ANN at score-level	CSIP: d' is 2.501, AUC is 0.943, EER is 0.131
(Jain et al., 2015)	Iris, Periocular: LBP, SIFT, GIST Fusion: Feature-level (context-switching), score-level (sum)	UBIRISv2: RR-10 is 76.16 % FRGC: RR-10 is 75.4 %
(Alonso-Fernandez et al., 2015)	Iris: Log-Gabor filters, DCT, SIFT Periocular: Symmetry patterns, gabor features, SIFT Fusion: Logistic regression at score-level	(EER) BioSec: 0.75%, MobBIO: 6.75% CASIA-Iris Inverval v3: 0.51% IIT Delhi v1.0: 0.38%, UBIRIS v2: 15.17%
(Verma et al., 2016)	Iris: Gabor features, Periocular: PHOG, GIST Fusion: Random decision forest at score-level	CASIA-IrisV4-distance: GMR is 61% at 0.1% FMR FOCS: GMR is 21% at 0.1% FMR
(Ahuja et al., 2016b)	Iris: RootSIFT, Periocular: Deep features Fusion: Mean rule and linear regression at score-level	MICHE-II: AUC is 0.985 and EER is 0.057
(Ahmed et al., 2017)	Iris: Gabor features, Periocular: Multi-Block Transitional LBP Fusion: Weighted sum rule at score-level	MICHE II: EER is 1.22%, FRR is 2.56% at FAR RR is 100%
(Zhang et al., 2018)	Iris, Periocular: CNNs with max out units Fusion: Weighted concatenation at the feature-level	CASIA-Iris-MobileV1.0: EER is 0.60%, FNMR is 2.32% at 0.001% FMR
(Silva et al., 2018)	Iris, Periocular: Deep features Fusion: Particle swarm optimization at feature-level	UBIRISv2: d' is 3.45 and EER is 5.55%
Fusion of Periocular and Face		
(Jillela and Ross, 2012)	Face: Verilook and PittPatt Scores, Ocular: SIFT, LBP Fusion: Mean rule at score-level fusion	Plastic surgery database: RR is 87.4%
(Pereira and Marcel, 2015)	Periocular: Tessellated images + DCT + GMM Face: Inter-session variability modeling + GMM Fusion: Linear logistic regression at score-level fusion	MOBIO: HTER is 6.58% CPqD Biometric: HTER is 3.87%
(Raja et al., 2015b)	Iris: Gabor features, Periocular, Face: SIFT, SURF, BSIF Fusion: Min, max, product, weighted sum at score-level	Proprietary: EER of 0.68%
(Stokkenes et al., 2017)	Face, Periocular: BSIF + Bloom filters Fusion: XOR operation, concatenation at feature-level	Proprietary: GMR is 88.54% at 0.01% FMR EER is 2.05%

Alonso-Fernandez et al., 2020). Table 5 provides a brief description of various mobile-based periocular recognition techniques.

8. Specific Applications

1. **Soft-biometrics from Periocular Region:** Soft-biometrics refer to attributes used to classify individuals in broad categories such as gender, ethnicity, race, age, height, weight, or hair color. The periocular region has also been used for automatically estimating age, gender, ethnicity, and facial expression information. An exploration of gender information contained in the periocular region is performed in (Merkow et al., 2010; Lyle et al., 2012; Bobeldyk and Ross, 2016; Castrilln-Santana et al., 2016; Tapia and Arellano, 2019). Tapia and Arellano (2019) synthesized NIR periocular images using a conditional GAN based on gender information, and then identify gender using the synthesized periocular images. The work in (Lyle et al., 2012; Woodard et al., 2017) extracted race information from the periocular region, while the work in (Rattani et al., 2017) determined an individual’s age from the periocular region. Alonso-Fernandez et al. (2018) investigated the feasibility of using the periocular region for facial expression recognition.
2. **Long Distance Recognition:** Bharadwaj et al. (2010) showed the degradation of iris recognition performance with an increase in standoff distance and suggested the use of the periocular region on long-distance images. The authors in (Tan and Kumar, 2012; Verma et al., 2016) proposed fusion approaches (iris and periocular) for human recognition at a distance (NIR images). Kim et al. (2018) presented CNN-based periocular recognition in a surveillance environment.
3. **Face Generation from Periocular Region:** Juefei-Xu et al. (2014); Juefei-Xu and Savvides (2016) recreated the entire face from the periocular region alone using dictionary learning algorithms, while Ud Din et al. (2020) proposed a GAN-based method to regenerate the masked part of the face. Li et al. (2020) utilized de-occlusion distillation framework to recover face content under the mask.
4. **Cross-modal Recognition (Face and Iris):** Jillela and Ross (2014) presented the challenging problem of matching face in VIS spectrum against iris images in NIR spectrum (cross-modal) using periocular information. They utilized LBP, Normalized Gradient Correlation (NGC), and Joint Dictionary-based Sparse Representation (JDSR) methods to accomplish cross-modality matching.
5. **Periocular Forensics:** The authors in (Marra et al., 2018; Banerjee and Ross, 2018) deduced sensor information from the periocular images. In another work, Banerjee and Ross (2019) suppressed the sensor-specific information (sensor anonymization) and also incorporated the sensor pattern of a different device (sensor spoofing) in periocular images.
6. **Other Applications:** Du et al. (2016) utilized the periocular region to correct mislabeled left and right iris images

in a diverse set of iris datasets. The work in (Alonso-Fernandez and Bigun, 2014; Hoffman et al., 2019) suggested the use of periocular information for iris spoof detection. Alonso-Fernandez and Bigun (2014) detected iris spoofs using VIS periocular images, whereas Hoffman et al. (2019) utilized NIR periocular images. Patel et al. (2017) explored the effectiveness of periocular region in verifying kinship using a Block-based Neighborhood Repulsed Metric Learning framework. Juefei-Xu et al. (2011) presented a framework of utilizing the periocular region for age invariant face recognition. The authors applied Walsh-Hadamard transform encoded Local Binary Patterns (WLBP) and Unsupervised Discriminant Projection (UDP), and achieved 100% rank-1 identification rate on a dataset of 82 subjects. The authors in (Jillela and Ross, 2012; Raja et al., 2016a) utilized the periocular region to identify individuals after they undergo facial plastic surgery. Mahalingam et al. (2014) introduced a medically altered gender transformation face dataset and proposed the fusion of periocular (patched-based LBP) with face, which outperformed standalone commercial-off-the-shelf face matchers. Keshari et al. (2016) investigated periocular recognition on pre- and post-cataract surgery images.

9. Datasets and Competitions

In early literature, periocular recognition was performed using face and iris datasets as there were limited datasets available that contained the periocular region only. Commonly used face datasets to perform periocular recognition research on VIS images are FRGC, FERET, FG-NET, MobBIO, and on NIR images are IIT Delhi v1.0, CASIA Interval, BioSec. The iris datasets used for periocular recognition research are UBIRIS v2 (VIS), MBGC (NIR), and PolyU cross-spectral datasets. Table 6 describes the datasets specifically collected for periocular recognition. Figures 4, 5, and 6 show a few images from these periocular datasets. The datasets used to perform periocular recognition research under variable stand-off distance are FRGC, UBIRIS v2, and UBIPr. Examples of datasets providing video data of subjects for periocular biometrics research are MBGC, FOCS, and VSSIRIS. Other datasets provide special evaluation scenarios such as aging (MORPH, FG-NET), plastic surgery (Raja et al., 2016a), gender transformation (Mahalingam et al., 2014), expression changes (FaceExpressUBI), face occlusion (AR, Compass), cross-spectral matching (CMU-H, IMP, CROSS-EYED 2016, CROSS-EYED 2017), or mobile authentication (CASIA-Iris-Mobile-V1.0, CSIP, MICHE I and II, VSSIRIS, VISOB 1.0 and 2.0, CMPD). Various competitions focusing on periocular recognition can be found in (Rattani et al., 2016; Sequeira et al., 2016; De Marsico et al., 2017; Sequeira et al., 2017). The competitions in (Rattani et al., 2016; De Marsico et al., 2017) are on mobile periocular images, while the competitions in (Sequeira et al., 2016; Sequeira et al., 2017) evaluated the cross-spectrum (matching of VIS and NIR images) scenario. Table 7 summarizes details about these competitions. Zanolrensi et al. (2021) surveyed various ocular datasets

Table 5. A chronological overview (description, datasets, and performance) of periocular techniques utilizing images acquired using the sensors and cameras in a mobile device such as a smartphone. Here, HTER is Half Total Error Rate. The acronyms used in the ‘Description’ column are defined in the text or in the referenced papers.

Paper	Description	Datasets and Performance
(Juefei-Xu and Savvides, 2012)	Walsh-Hadamard transform encoded LBP + Kernel class-dependence feature analysis	Compass: GAR is 60.7% at 0.1% FAR
(Raja et al., 2014b)	SIFT, SURF and BSIF + Nearest Neighbors (SIFT and SURF), Bhattacharyya distance(BSIF)	Proprietary: GAR is 89.38% at 0.01% FAR
(Ahuja et al., 2016a)	SURF + Multinomial Naive Bayes learning + Pyramid-up topology using Dense SIFT + RANSAC	VISOB: RR is 48.76%-79.49%
(Keshari et al., 2016)	Dense SIFT, Gabor, Scattering Network features + PCA + LDA + Cosine similarity weighted sum	IMP: RR-10 is 69% GAR is 24% at 1% FAR
(Raghavendra and Busch, 2016)	Maximum Response filters + Deeply coupled autoencoders	VISOB: GMR of 93.98% at 0.001 FMR
(Raja et al., 2016c)	Laplacian decomposition + GLCM + STFT + Histogram features of freq. response + SRC	MICHE I: Cross-camera EER is 7.53% Cross-sensor EER is 6.38%
(Ahuja et al., 2017)	Hybrid CNN model + Mean fusion at the score-level	VISOB: GMR is 99.5% at 0.001% FMR MICHE-II: AUC of 98.6%
(Rattani and Derakhshani, 2017)	Fine-tuned VGG-16, VGG-19, InceptionNet, ResNet	VISOB: TMR is 100% at 0.001% FMR
(Garg et al., 2018)	Heterogeneity aware loss function in deep network	(RR) CSIP (cross-sensor): 89.53%, IMP: 61.20%, VISOB (cross-spectrum): 99.41%
(Reddy et al., 2018b)	Patch-based OcularNet	(EER) VISOB: 1.17%, UBIRIS-I: 9.86%, UBIRIS-II: 9.77%, CROSS-EYED2016: 14.95%
(Raja et al., 2020)	Deep Sparse Features, Deep Sparse Time Frequency Features + CRC classification	(GMR at 0.01% FMR) VISPI: 99.80%, MICHE-I: 100%, VISOB: 98.78%
(Boutros et al., 2020)	Periocular, Iris: Hand-crafted and deep features + Synthesize identity-preserved periocular images	OpenEDS: EER (iris) is 6.35% EER (periocular) is 5.86%

and discussed popular ocular recognition competitions. The authors described 36 iris, 4 iris/periocular, 4 periocular, and 10 multimodal datasets.

10. Challenges and Future Directions

- 1. Definition and Standardization:** The definition of the periocular region is not standardized. What is the actual boundary around the eye? Should we consider a single eye or both eyes to be in the periocular region? These questions about the scope of the periocular region is yet to be answered. Apart from these definitional concerns, issues around standardization has to be resolved for ground-truth segmentation, and the minimum resolution needed for recognition.
- 2. Generalizability:** Periocular biometric solutions should be generalizable, which refers to the matching of periocular images under cross-sensor (images from different sensors), cross-spectrum (images from different spectra), cross-dataset (images from different datasets), cross-resolution (images at multiple distances), and cross-modal (images from different modalities) scenarios.
- 3. Non-ideal Conditions:** Researchers need to focus on periocular matching under non-ideal conditions, i.e., pose variations (Park et al., 2011; Karakaya, 2021), expression, non-uniform illumination, low-resolution, occlusions (eyeglasses, eye-blinking, different types of masks, scarfs or helmets or eye makeup), or large stand-off distance.
- 4. Effects of Aging:** With age, wrinkles and folds around the eye could change the overall appearance of the periocular region. The effects of aging on periocular recognition are yet to be comprehensively studied (Ma et al., 2019).

- 5. Anti-spoofing Measures:** While periocular region has been utilized to detect iris spoof attacks (Alonso-Fernandez and Bigun, 2014; Hoffman et al., 2019), we should also be vigilant about spoof attacks directed at the periocular region.
- 6. Explainability and Interpretability:** Increasing use of deep learning-based techniques in periocular biometrics opens another direction which involves explainability of these deep learning models (Brito and Proena, 2021).

11. Summary

This article provided a survey on periocular biometrics in the wake of its importance due to the increased use of face masks. Firstly, we reported recent face and periocular recognition techniques specifically designed to recognize humans wearing a face mask. Subsequently, we provided details on various aspects of periocular biometrics, viz., anatomical cues in the periocular region used for recognition, various feature extraction and matching techniques, cross-spectral recognition, its fusion with other biometrics modalities (face or iris), authentication in mobile devices, usefulness of this biometric in other applications, periocular datasets, and competitions. Finally, we discussed the various challenges and future directions to work on. The applicability of the periocular biometrics is likely to extend to other scenarios where only the ocular region of the face may be visible. This could be due to cultural etiquette (e.g., women covering their face) or safety precautions (e.g., surgeons or construction workers covering their nose and mouth).

Table 6. Description of periocular datasets (NIR, VIS, and multi-spectrum), along with representative research papers utilizing these datasets.

Datasets	Description	Papers
NIR Spectrum		
NIST- Face and ocular challenge series (FOCS)	9,588 total images, 136 subjects, 750x600 resolution, monocular images IOM sensor	(Boddeti et al., 2011; Ross et al., 2012; Monwar et al., 2013) (Smereka and Kumar, 2013; Smereka et al., 2015) (Verma et al., 2016; Zhao and Kumar, 2017)
MIR 2016 (Zhang et al., 2016)	16,500 total images, 550 subjects, 1968x2014 resolution, biocular images IrisKing mobile sensor	(Zhang et al., 2016)
CASIA-Iris-Mobile-V1.0 (Zhang et al., 2018)	11,000 total images, 630 subjects, biocular images, CASIA NIR mobile camera	(Zhang et al., 2018)
CASIA-IrisV4-Distance	2,567 total images, 142 subjects, 2352x1728 resolution, biocular images, CASIA long-range iris camera	(Tan and Kumar, 2012, 2013; Verma et al., 2016)
Visible Spectrum		
UBIPr (Padole and Proena, 2012)	10,950 total images, 261 subjects, Canon EOS 5D, biocular images	(Padole and Proena, 2012; Nie et al., 2014; Hernandez-Diaz et al., 2018) (Smereka et al., 2015; Reddy et al., 2019, 2020)
CSIP (Santos et al., 2015)	2,004 total images, 50 subjects, monocular images 4 mobile sensors (Xperia Arc S, Apple iPhone4, THL W200, Huawei U8510)	(Santos et al., 2015; Garg et al., 2018)
MICHE I (De Marsico et al., 2015)	3,732 total images, 92 subjects, monocular images 3 mobile sensors (iPhone5, Galaxy Samsung IV, Galaxy Tablet II)	(De Marsico et al., 2015; Raja et al., 2016c; Reddy et al., 2019; Raja et al., 2020)
VSSIRIS (Raja et al., 2015)	560 total images, 28 subjects, monocular images 2 mobile sensors (iPhone 5S and Nokia Lumia 1020)	(Raja et al., 2015; Alonso-Fernandez et al., 2020)
VISOB v1.0(Rattani et al., 2016)	158,136 total images, 550 subjects, monocular images 3 mobile sensors (iPhone 5s, Samsung Note 4 and Oppo N1)	(Ahuja et al., 2016a; Raghavendra and Busch, 2016; Ahuja et al., 2017) (Garg et al., 2018; Hoang et al., 2020; Raja et al., 2020; Reddy et al., 2020)
CMPD (Keshari et al., 2016)	2,380 total images, 56 subjects, monocular images MicroMax A350 Canvas Knight mobile device	(Keshari et al., 2016)
MICHE II (De Marsico et al., 2017)	3,120 total images, 75 subjects, monocular images, 3 mobile sensors (iPhone5, Galaxy Samsung IV, Galaxy Tablet II)	(Ahuja et al., 2016b; Ahmed et al., 2017) (Ahuja et al., 2017; De Marsico et al., 2017)
UFPR-Periocular (Zanlorensi et al., 2020)	33,660 total images, 1,122 subjects, both monocular and biocular images 196 mobile sensors	(Zanlorensi et al., 2020)
VISOB 2.0	75,428 total images, 250 subjects, monocular images 2 mobile sensors (Samsung Note 4 and Oppo N1)	(Krishnan et al., 2020)
Multi-spectrum		
IMP (Sharma et al., 2014)	1,240 total images, 62 subjects, monocular and biocular images 3 sensors (Cogent iris scanner, Sony HandyCam, Nikon SLR camera)	(Keshari et al., 2016; Ramaiah and Kumar, 2016; Algashaam et al., 2017a) (Behera et al., 2017; Garg et al., 2018; Hernandez-Diaz et al., 2019) (Behera et al., 2020; Ipe and Thomas, 2020)
CROSS-EYED 2016 (Sequeira et al., 2016)	3,840 total images, 120 subjects, 900800 resolution, monocular images	(Behera et al., 2017; Raja et al., 2017; Reddy et al., 2018b) (Alonso-Fernandez et al., 2020; Behera et al., 2020; Reddy et al., 2020)
CROSS-EYED 2017 (Sequeira et al., 2017)	5,600 total images, 175 subjects, 900800 resolution, monocular images	(Sequeira et al., 2017)
QUT Multispectral (Algashaam et al., 2017a)	212 total images, 53 subjects, 800x600 resolution, biocular images 2 sensors (Sony DCR-DVD653E, IP2M-842B Surveillance camera)	(Algashaam et al., 2017a)

Table 7. A summary (datasets and performance achieved) of various competitions on periocular recognition. Here, GFRR is Generalized False Rejection Rate, and GFAR is Generalized False Acceptance Rate.

Competition	Dataset	Performance
MICHE-II (De Marsico et al., 2017)	MICHE-I and MICHE-II	EER is 2.74% and FRR is 9.13% @ 0.1% FAR (Ahmed et al., 2016; Ahmed et al., 2017)
ICIP (Rattani et al., 2016)	VISOB	EER is 0.06% - 0.20% and GMR is 92% @ 0.1% FMR (Raghavendra and Busch, 2016)
CROSS-EYED 2016 (Sequeira et al., 2016)	CROSS-EYED 2016	GFRR is 0.0% @ 1% GFAR and EER is 0.29% (HH1) (Sequeira et al., 2016)
CROSS-EYED 2017 (Sequeira et al., 2017)	CROSS-EYED 2016 and 2017	GFRR is 0.74% @ 1% GFAR and EER is 0.82% (HH1) (Sequeira et al., 2017)

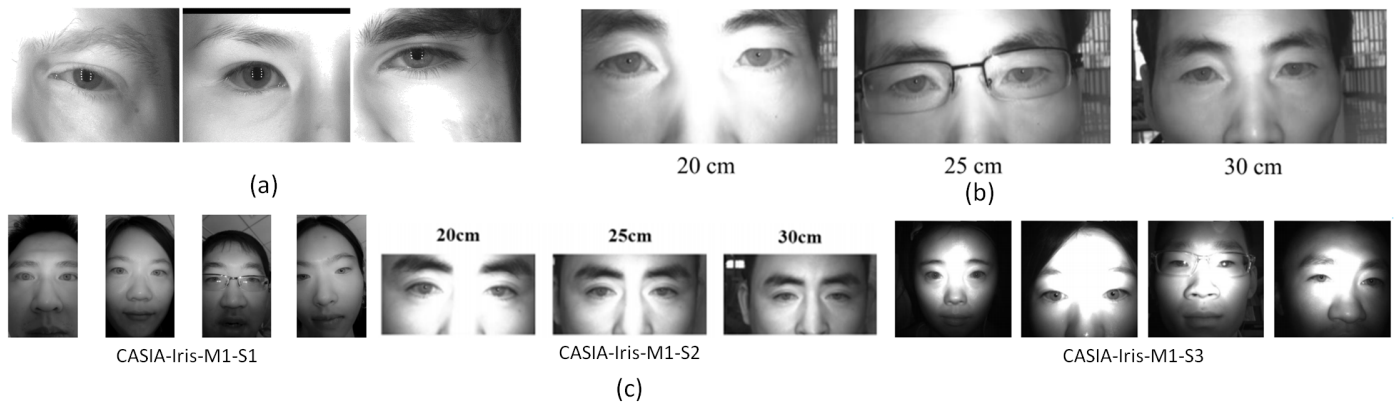


Fig. 4. Examples of periocular images from NIR datasets: (a) FOCUS Dataset, (b) MIR 2016 Dataset (Zhang et al., 2016), (c) CASIA-Iris-Mobile-V1.0 Dataset (Zhang et al., 2018).

References

- Adams, J., Woodard, D.L., Dozier, G., Miller, P., Bryant, K., Glenn, G., 2010. Genetic-based type II feature extraction for periocular biometric recognition: Less is more. *International Conference on Pattern Recognition (ICPR)*, 205–208.
- Ahmed, N.U., Cvetkovic, S., Siddiqi, E.H., Nikiforov, A., Nikiforov, I., 2016. Using fusion of iris code and periocular biometric for matching visible spectrum iris images captured by smart phone cameras. *International Conference on Pattern Recognition (ICPR)*, 176–180.
- Ahmed, N.U., Cvetkovic, S., Siddiqi, E.H., Nikiforov, A., Nikiforov, I., 2017. Combining iris and periocular biometric for matching visible spectrum eye images. *Pattern Recognition Letters (PRL)* 91, 11–16.
- Ahuja, K., Bose, A., Nagar, S., Dey, K., Barbhuiya, F., 2016a. Isure: User authentication in mobile devices using ocular biometrics in visible spectrum. *International Conference on Image Processing (ICIP)*, 335–339.
- Ahuja, K., Islam, R., Barbhuiya, F.A., Dey, K., 2016b. A preliminary study of CNNs for iris and periocular verification in the visible spectrum. *International Conference on Pattern Recognition (ICPR)*, 181–186.
- Ahuja, K., Islam, R., Barbhuiya, F.A., Dey, K., 2017. Convolutional neural networks for ocular smartphone-based biometrics. *Pattern Recognition Letters (PRL)* 91, 17–26.
- Alghashaam, F., Nguyen, K., Banks, J., Chandran, V., Do, T.A., Alkanhal, M., 2021. Hierarchical fusion network for periocular and iris by neural network approximation and sparse autoencoder. *Machine Vision and Applications* 32 (2021).
- Alghashaam, F.M., Nguyen, K., Alkanhal, M., Chandran, V., Boles, W., Banks, J., 2017a. Multispectral periocular classification with multimodal compact multi-linear pooling. *IEEE Access*, 14572–14578.
- Alghashaam, F.M., Nguyen, K., Chandran, V., Banks, J., 2017b. Elliptical higher-order-spectra periocular code. *IEEE Access* 5, 6978–6988.
- Alonso-Fernandez, F., Bigun, J., 2012. Periocular recognition using retinotopic sampling and Gabor decomposition. *Computer Vision – ECCV Workshops and Demonstrations*, 309–318.
- Alonso-Fernandez, F., Bigun, J., 2014. Best regions for periocular recognition with NIR and visible images. *International Conference on Image Processing (ICIP)*, 4987–4991.
- Alonso-Fernandez, F., Bigun, J., 2014. Exploring periocular and RGB information in fake iris detection. *International Convention on Information and Communication Technology, Electronics and Microelectronics (MIPRO)*, 1354–1359.
- Alonso-Fernandez, F., Bigun, J., 2015. Near-infrared and visible-light periocular recognition with Gabor features using frequency-adaptive automatic eye detection. *IET Biometrics* (2015) 4.
- Alonso-Fernandez, F., Bigun, J., 2016. A survey on periocular biometrics research. *Pattern Recognition Letters (PRL)* 82, 92–105.
- Alonso-Fernandez, F., Bigun, J., Englund, C., 2018. Expression recognition using the periocular region: A feasibility study. *International Conference on Signal-Image Technology Internet-Based Systems (SITIS)*, 536–541.
- Alonso-Fernandez, F., Mikaelyan, A., Bigun, J., 2015. Comparison and fusion of multiple iris and periocular matchers using near-infrared and visible images. *International Workshop on Biometrics and Forensics (IWBF)*, 1–6.
- Alonso-Fernandez, F., Raja, K.B., Raghavendra, R., Busch, C., Bigun, J., Vera-Rodriguez, R., Fierrez, J., 2020. Cross-sensor periocular biometrics for partial face recognition in a global pandemic: Comparative benchmark and novel multialgorithmic approach. *arXiv:1902.08123*.
- Ambika, D., Radhika, K., Seshachalam, D., 2016. Periocular authentication based on FEM using LaplaceBeltrami eigenvalues. *Pattern Recognition (PR)* 50, 178–194.
- Anwar, A., Raychowdhury, A., 2020. Masked face recognition for secure authentication. *arXiv:2008.11104*.
- Badejo, J., Akinrinmade, A., Adetiba, E., 2019. Survey of periocular recognition techniques. *Journal of Engineering Science and Technology Review* 12, 214–226.
- Bakshi, S., Sa, P., Majhi, B., 2013. Optimized periocular template selection for human recognition. *BioMed research international*, 481431.
- Bakshi, S., Sa, P., Wang, H., BARPANDA, S., Majhi, B., 2018. Fast periocular authentication in handheld devices with reduced phase intensive local pattern. *Multimedia Tools and Applications (MTA)* 77 (2018).
- Bakshi, S., Sa, P.K., Majhi, B., 2014. Phase intensive global pattern for periocular recognition. *Annual IEEE India Conference (INDICON)*, 1–5.
- Bakshi, S., Sa, P.K., Majhi, B., 2015. A novel phase-intensive local pattern for periocular recognition under visible spectrum. *BioCybernetics and Biomedical Engineering* 35, 30–44.
- Banerjee, S., Ross, A., 2018. Impact of photometric transformations on PRNU estimation schemes: A case study using near infrared ocular images. *International Workshop on Biometrics and Forensics (IWBF)*, 1–8.
- Banerjee, S., Ross, A., 2019. Smartphone camera de-identification while preserving biometric utility. *International Conference on Biometrics Theory, Applications and Systems (BTAS)*, 1–10.
- Behera, S.S., Gour, M., Kanhangad, V., Puhan, N., 2017. Periocular recognition in cross-spectral scenario. *International Joint Conference on Biometrics (IJCB)*, 681–687.
- Behera, S.S., Mandal, B., Puhan, N.B., 2019. Cross-spectral periocular recognition: A survey, in: Sridhar, V., Padma, M., Rao, K.R. (Eds.), *Emerging Research in Electronics, Computer Science and Technology*, Springer Singapore. pp. 731–741.
- Behera, S.S., Mishra, S.S., Mandal, B., Puhan, N.B., 2020. Variance-guided attention-based twin deep network for cross-spectral periocular recognition. *Image and Vision Computing (IVC)* 104, 104016.
- Beom-Seok Oh, Kangrok Oh, Kar-Ann Toh, 2012. On projection-based methods for periocular identity verification. *Conference on Industrial Electronics and Applications (ICIEA)*, 871–876.
- Bharadwaj, S., Bhatt, H.S., Vatsa, M., Singh, R., 2010. Periocular biometrics: When iris recognition fails. *International Conference on Biometrics: Theory, Applications and Systems (BTAS)*, 1–6.
- Bobeldyk, D., Ross, A., 2016. Iris or periocular? exploring sex prediction from near infrared ocular images. *International Conference of the Biometrics Special Interest Group (BIOSIG)*, 1–7.
- Boddeti, V.N., Smereka, J.M., Vijaya Kumar, B.V.K., 2011. A comparative evaluation of iris and ocular recognition methods on challenging ocular images. *International Joint Conference on Biometrics (IJCB)*, 1–8.
- Boutros, F., Damer, N., Kirchbuchner, F., Kuijper, A., 2021a. Self-restrained

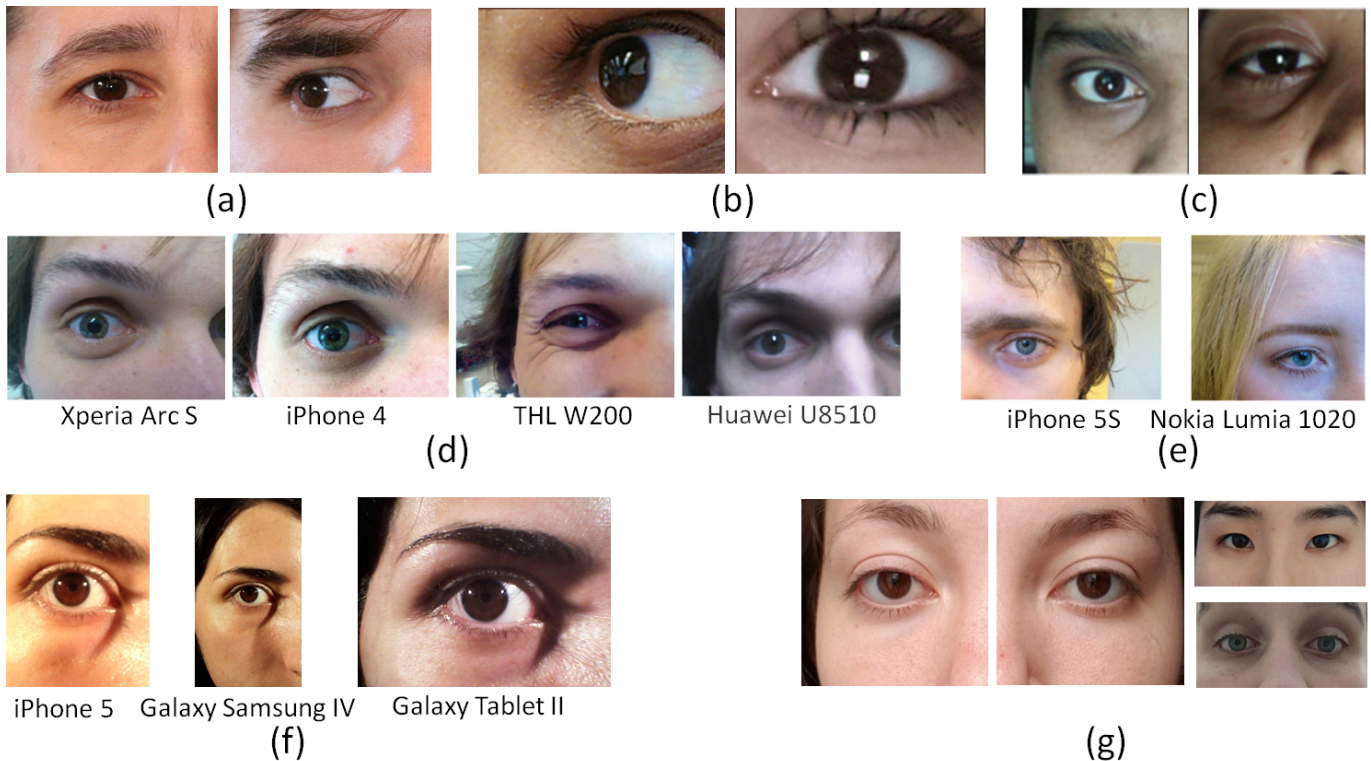


Fig. 5. Examples of periocular images from VIS datasets: (a) UBIPr dataset (Padole and Proena, 2012), (b) VISOB 1.0 Dataset (Rattani et al., 2016), (c) VISOB 2.0 Dataset, (d) CSIP Dataset (Santos et al., 2015), (e) VSSIRIS Dataset (Raja et al., 2015), (f) MICHE-I Dataset (De Marsico et al., 2015), (g) UFPR-Periocular (Zanlorensi et al., 2020).

- triplet loss for accurate masked face recognition. arXiv:2103.01716 .
- Boutros, F., Damer, N., Kolf, J.N., Raja, K.B., Kirchbuchner, F., Ramachandra, R., Kuijper, A., Fang, P., Zhang, C., Wang, F., Montero, D., Aginako, N., Sierra, B., Nieto, M., Erakin, M.E., Demir, U., Ekenel, H.K., Kataoka, A., Ichikawa, K., Kubo, S., Zhang, J., He, M., Han, D., Shan, S., Grm, K., Struc, V., Seneviratne, S., Kasthuriarachchi, N., Rasnayaka, S., Neto, P.C., Sequeira, A.F., Pinto, J.R., Saffari, M., Cardoso, J.S., 2021b. MFR 2021: masked face recognition competition. *International Joint Conference on Biometrics (IJCB)*, 1–10.
- Boutros, F., Damer, N., Raja, K., Ramachandra, R., Kirchbuchner, F., Kuijper, A., 2020. Iris and periocular biometrics for head mounted displays: Segmentation, recognition, and synthetic data generation. *Image and Vision Computing (IVC)* 104, 104007.
- Bowyer, K., Hollingsworth, K., Flynn, P., 2013. A survey of iris biometrics research: 2008–2010, in: M., B., K., B. (Eds.), *Handbook of Iris Recognition*, Advances in Computer Vision and Pattern Recognition. Springer, London.
- Bowyer, K.W., Hollingsworth, K., Flynn, P.J., 2008. Image understanding for iris biometrics: A survey. *Computer Vision and Image Understanding (CVIU)* 110, 281 – 307.
- Brito, J., Proena, H., 2021. A short survey on machine learning explainability: An application to periocular recognition. *Electronics* 10 (2021).
- Cantoni, V., Galdi, C., Nappi, M., Porta, M., Riccio, D., 2015. GANT: Gaze analysis technique for human identification. *Pattern Recognition (PR)* 48, 1027 – 1038.
- Cao, Z.X., Schmid, N.A., 2014. Matching heterogeneous periocular regions: Short and long standoff distances. *International Conference on Image Processing (ICIP)*, 4967–4971.
- CASIA-IrisV4-Distance, . <https://hycasia.github.io/dataset/casia-irisv4/>.
- Castrilln-Santana, M., Lorenzo-Navarro, J., Ramn-Balmaseda, E., 2016. On using periocular biometric for gender classification in the wild. *Pattern Recognition Letters (PRL)* 82, 181 – 189.
- Chen, L., Ferryman, J., 2015. Combining 3D and 2D for less constrained periocular recognition. *International Conference on Biometrics Theory, Applications and Systems (BTAS)*, 1–6.
- Chowdary, G.J., Punn, N.S., Sonbhadra, S.K., Agarwal, S., 2020. Face mask detection using transfer learning of inceptionv3. *Lecture Notes in Computer Science*, 8190.
- Crihalmeanu, S., Ross, A., 2012. Multispectral scleral patterns for ocular biometric recognition. *Pattern Recognition Letters (PRL)* 33, 1860 – 1869.
- Damer, N., Boutros, F., Süßmilch, M., Fang, M., Kirchbuchner, F., Kuijper, A., 2021. Masked face recognition: Human vs. machine. arXiv:2103.01924 .
- Damer, N., Grebe, J.H., Chen, C., Boutros, F., Kirchbuchner, F., Kuijper, A., 2020. The effect of wearing a mask on face recognition performance: an exploratory study. *International Conference of the Biometrics Special Interest Group (BIOSIG)*, 1–6.
- Das, A., Pal, U., Blumenstein, M., Ballester, M.A.F., 2013. Sclera recognition - a survey. *IAPR Asian Conference on Pattern Recognition (ACPR)*, 917–921.
- De Marsico, M., Nappi, M., Proena, H., 2017. Results from MICHE II Mobile Iris CHallenge Evaluation II. *Pattern Recognition Letters (PRL)* 91, 3 – 10.
- De Marsico, M., Nappi, M., Riccio, D., Wechsler, H., 2015. Mobile Iris Challenge Evaluation (MICHE)-I: biometric iris dataset and protocols. *Pattern Recognition Letters (PRL)* 57, 17 – 23.
- Deng, J., Guo, J., An, X., Zhu, Z., Zafeiriou, S., 2021. Masked face recognition challenge: The InsightFace track report. *IEEE International Conference on Computer Vision Workshops (ICCV-W)*, 1437–1444.
- Derakhshani, R., Ross, A., 2007. A texture-based neural network classifier for biometric identification using ocular surface vasculature. *International Joint Conference on Neural Networks (IJCNN)*, 2982–2987.
- Ding, F., Peng, P., Huang, Y., Geng, M., Tian, Y., 2020. Masked face recognition with latent part detection. *ACM International Conference on Multimedia (MM)*, 22812289.
- Dong, Y., Woodard, D.L., 2011. Eyebrow shape-based features for biometric recognition and gender classification: A feasibility study. *International Joint Conference on Biometrics (IJCB)*, 1–8.
- Du, Y., Bourlai, T., Dawson, J., 2016. Automated classification of mislabeled near-infrared left and right iris images using convolutional neural networks. *International Conference on Biometrics Theory, Applications and Systems (BTAS)*, 1–6.
- FOCS, . <https://www.nist.gov/programs-projects/face-and-ocular-challenge-series-focs>.

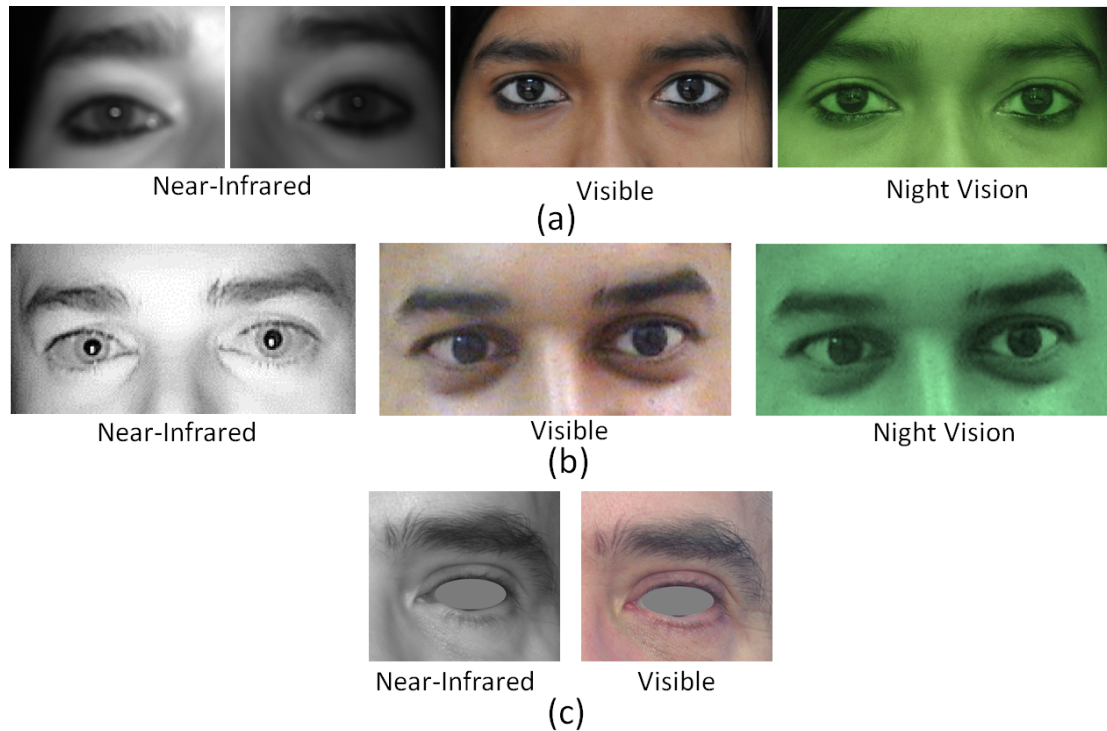


Fig. 6. Examples of periocular images from Multi-spectral datasets: (a) IIITD Multispectral Periocular (IMP) (Sharma et al., 2014), (b) QUT Multispectral (Algashaam et al., 2017a), and (c) Cross-Eyed 2016 (Sequeira et al., 2016).

- Garg, R., Baweja, Y., Ghosh, S., Singh, R., Vatsa, M., Ratha, N., 2018. Heterogeneity aware deep embedding for mobile periocular recognition. *International Conference on Biometrics Theory, Applications and Systems (BTAS)*, 1–7.
- Ge, S., Li, J., Ye, Q., Luo., Z., 2017. Detecting masked faces in the wild with LLE-CNNs. *Computer Vision and Pattern Recognition (CVPR)*, 426–434.
- Geng, M., Peng, P., Huang, Y., Tian, Y., 2020. Masked face recognition with generative data augmentation and domain constrained ranking. *ACM International Conference on Multimedia (MM)*, 22462254.
- Hariri, W., 2021. Efficient masked face recognition method during the COVID-19 pandemic. *arXiv:2105.03026*.
- Hernandez-Diaz, K., Alonso-Fernandez, F., Bigun, J., 2018. Periocular recognition using CNN features off-the-shelf. *International Conference of the Biometrics Special Interest Group (BIOSIG)*, 1–5.
- Hernandez-Diaz, K., Alonso-Fernandez, F., Bigun, J., 2019. Cross spectral periocular matching using ResNet features. *International Conference on Biometrics (ICB)*, 1–7.
- Hernandez-Diaz, K., Alonso-Fernandez, F., Bigun, J., 2020. Cross-spectral periocular recognition with conditional adversarial networks. *International Joint Conference on Biometrics (IJCB) (2020)*.
- Hoang, N., Rattani, A., Derakhshani, R., 2020. Eyebrow deserves attention: Upper periocular biometrics. *International Conference of the Biometrics Special Interest Group (BIOSIG)*, 1–5.
- Hoffman, S., Sharma, R., Ross, A., 2019. Iris + ocular: Generalized iris presentation attack detection using multiple convolutional neural networks. *International Conference on Biometrics (ICB)*, 1–8.
- Holland, C.D., Komogortsev, O.V., 2013. Complex eye movement pattern biometrics: The effects of environment and stimulus. *IEEE Transactions on Information Forensics and Security (TIFS)* 8, 2115–2126.
- Hollingsworth, K., Bowyer, K.W., Flynn, P.J., 2010. Identifying useful features for recognition in near-infrared periocular images. *International Conference on Biometrics: Theory, Applications and Systems (BTAS)*, 1–8.
- Hollingsworth, K., Bowyer, K.W., Flynn, P.J., 2011. Useful features for human verification in near-infrared periocular images. *Image and Vision Computing (IVC)* 29, 707 – 715.
- Hollingsworth, K.P., Darnell, S.S., Miller, P.E., Woodard, D.L., Bowyer, K.W., Flynn, P.J., 2012. Human and machine performance on periocular biometrics under near-infrared light and visible light. *IEEE Transactions on Information Forensics and Security (TIFS)* 7, 588–601.
- Hwang, H., Lee, E.C., 2020. Near-infrared image-based periocular biometric method using convolutional neural network. *IEEE Access* 8, 158612–158621.
- Ipe, V.M., Thomas, T., 2020. CNN based periocular recognition using multi-spectral images, in: Thampi, S.M., Hegde, R.M., Krishnan, S., Mukhopadhyay, J., Chaudhary, V., Marques, O., Piramuthu, S., Corchado, J.M. (Eds.), *Advances in Signal Processing and Intelligent Recognition Systems*, Springer Singapore. pp. 94–105.
- Jain, A., Mittal, P., Goswami, G., Vatsa, M., Singh, R., 2015. Person identification at a distance via ocular biometrics. *International Conference on Identity, Security and Behavior Analysis (ISBA)*, 1–6.
- Jain, A.K., Ross, A.A., Nandakumar, K., 2011. *Introduction to Biometrics*. Springer Publishers.
- Jillela, R., Ross, A., 2012. Mitigating effects of plastic surgery: Fusing face and ocular biometrics. *International Conference on Biometrics: Theory, Applications and Systems (BTAS)*, 402–411.
- Jillela, R., Ross, A., 2014. Matching face against iris images using periocular information. *International Conference on Image Processing (ICIP)*, 4997–5001.
- Joshi, A., Gangwar, A., Sharma, R., Singh, A., Saquib, Z., 2014. Periocular recognition based on Gabor and Parzen PNN. *International Conference on Image Processing (ICIP)*, 4977–4981.
- Juefei-Xu, F., Cha, M., Heyman, J.L., Venugopalan, S., Abiantun, R., Savvides, M., 2010. Robust local binary pattern feature sets for periocular biometric identification. *International Conference on Biometrics: Theory, Applications and Systems (BTAS)*, 1–8.
- Juefei-Xu, F., Cha, M., Savvides, M., Bedros, S., Trojanova, J., 2011. Investigating age invariant face recognition based on periocular biometrics. *International Joint Conference on Biometrics (IJCB)*, 1–7.
- Juefei-Xu, F., Pal, D.K., Savvides, M., 2014. Hallucinating the full face from the periocular region via dimensionally weighted K-SVD. *Conference on Computer Vision and Pattern Recognition Workshops (CVPR-W)*, 1–8.
- Juefei-Xu, F., Savvides, M., 2012. Unconstrained periocular biometric acquisition and recognition using COTS PTZ camera for uncooperative and non-cooperative subjects. *Workshop on the Applications of Computer Vision (WACV)*, 201–208.
- Juefei-Xu, F., Savvides, M., 2016. Fastfood dictionary learning for periocular-

- based full face hallucination. International Conference on Biometrics Theory, Applications and Systems (BTAS), 1–8.
- Jung, Y.G., Low, C.Y., Park, J., Teoh, A.B.J., 2020. Periocular recognition in the wild with generalized label smoothing regularization. *Signal Processing Letters (SPL)* 27, 1455–1459.
- Karahan, A., Karaz, A., Zdemir, F., G, A.G., Uludag, U., 2014. On identification from periocular region utilizing SIFT and SURF. *European Signal Processing Conference (EUSIPCO)*, 1392–1396.
- Karakaya, M., 2021. Iris-ocular-periocular: toward more accurate biometrics for off-angle images. *Journal of Electronic Imaging* 30, 1–21.
- Keshari, R., Ghosh, S., Agarwal, A., Singh, R., Vatsa, M., 2016. Mobile periocular matching with pre-post cataract surgery. *International Conference on Image Processing (ICIP)*, 3116–3120.
- Kim, M.C., Koo, J.H., Cho, S.W., Baek, N.R., Park, K.R., 2018. Convolutional neural network-based periocular recognition in surveillance environments. *IEEE Access* 6, 57291–57310.
- Komogortsev, O.V., Jayarathna, S., Aragon, C.R., Mahmoud, M., 2010. Biometric identification via an oculomotor plant mathematical model, in: *Proceedings of the 2010 Symposium on Eye-Tracking Research & Applications*, Association for Computing Machinery. p. 5760.
- Komogortsev, O.V., Karpov, A., Holland, C.D., Proena, H.P., 2012. Multimodal ocular biometrics approach: A feasibility study. *International Conference on Biometrics: Theory, Applications and Systems (BTAS)*, 209–216.
- Krishnan, A., Almadan, A., Rattani, A., 2020. Probing fairness of mobile ocular biometrics methods across gender on visob 2.0 dataset. *arXiv:2011.08898*.
- Kumari, P., Seeja, K., 2019. Periocular biometrics: A survey. *Journal of King Saud University - Computer and Information Sciences* (2019).
- Kumari, P., Seeja, K., 2020. Periocular biometrics for non-ideal images: with off-the-shelf deep CNN & transfer learning approach. *Procedia Computer Science* 167, 344–352.
- Kumari, P., Seeja, K.R., 2021a. A novel periocular biometrics solution for authentication during Covid-19 pandemic situation. *Journal of Ambient Intelligence and Humanized Computing*, 1032110337.
- Kumari, P., Seeja, K.R., 2021b. An optimal feature enriched region of interest (ROI) extraction for periocular biometric system. *Multimedia Tools and Applications (MTA)* (2021).
- Le, T.H.N., Prabhu, U., Savvides, M., 2014. A novel eyebrow segmentation and eyebrow shape-based identification. *International Joint Conference on Biometrics (IJCB)*, 1–8.
- Li, C., Ge, S., Zhang, D., Li, J., 2020. Look through masks: Towards masked face recognition with de-occlusion distillation. *ACM International Conference on Multimedia (MM)*, 30163024.
- Lin, C., Kumar, A., 2019. A CNN-based framework for comparison of contactless to contact-based fingerprints. *IEEE Transactions on Information Forensics and Security (TIFS)* 14, 662–676.
- Loey, M., Manogaran, G., Taha, M.H.N., Khalifa, N.E.M., 2021. A hybrid deep transfer learning model with machine learning methods for face mask detection in the era of the COVID-19 pandemic. *Measurement* 167, 108288.
- Luz, E., Moreira, G., Zanlorensi Junior, L.A., Menotti, D., 2018. Deep periocular representation aiming video surveillance. *Pattern Recognition Letters (PRL)* 114, 2–12.
- Lyle, J.R., Miller, P.E., Pundlik, S.J., Woodard, D.L., 2012. Soft biometric classification using local appearance periocular region features. *Pattern Recognition (PR)* 45, 3877–3885.
- Ma, H., Chen, Y., Cai, X., Tang, Z., Nie, C., Lu, R., 2019. Effect of aging in periocular appearances by comparison of anthropometry between early and middle adulthood in chinese han population. *Journal of Plastic, Reconstructive and Aesthetic Surgery* 72, 2002–2008.
- Mahalingam, G., Ricanek, K., Albert, A.M., 2014. Investigating the periocular-based face recognition across gender transformation. *IEEE Transactions on Information Forensics and Security (TIFS)* 9, 2180–2192.
- Marra, F., Poggi, G., Sansone, C., Verdoliva, L., 2018. A deep learning approach for iris sensor model identification. *Pattern Recognition Letters (PRL)* 113, 46–53.
- Merkow, J., Jou, B., Savvides, M., 2010. An exploration of gender identification using only the periocular region. *International Conference on Biometrics: Theory, Applications and Systems (BTAS)*, 1–5.
- Mikaelyan, A., Alonso-Fernandez, F., Bigun, J., 2014. Periocular recognition by detection of local symmetry patterns. *International Conference on Signal-Image Technology and Internet-Based Systems (SITIS)*, 584–591.
- Miller, P.E., Lyle, J.R., Pundlik, S.J., Woodard, D.L., 2010. Performance evaluation of local appearance based periocular recognition. *International Conference on Biometrics: Theory, Applications and Systems (BTAS)*, 1–6.
- Miller, P.E., Rawls, A.W., Pundlik, S.J., Woodard, D.L., 2010. Personal identification using periocular skin texture. *ACM Symposium on Applied Computing*, 14961500.
- Montero, D., Nieto, M., Leskovský, P., Aginako, N., 2021. Boosting masked face recognition with multi-task arcface. *arXiv:2104.09874*.
- Monwar, M.M., Vijayakumar, B.V.K., Boddeti, V.N., Smereka, J.M., 2013. Rank information fusion for challenging ocular image recognition. *International Conference on Cognitive Informatics and Cognitive Computing (IC-CICC)*, 175–181.
- Moreno, J.C., Surya Prasath, V.B., Santos, G., Proença, H., 2016. Robust periocular recognition by fusing sparse representations of color and geometry information. *International Journal of Signal Processing Systems (IJSPPS)* 82, 403417.
- Ngan, M., Grother, P., Hanaoka, K., 2020a. NISTIR 8311 - Ongoing FRVT Part 6A: Face recognition accuracy with face masks using pre-COVID-19 algorithms. *National Institute of Standards and Technology (NIST)* (2020).
- Ngan, M., Grother, P., Hanaoka, K., 2020b. NISTIR 8331 - Ongoing FRVT Part 6B: Face recognition accuracy with face masks using post-COVID-19 algorithms. *National Institute of Standards and Technology (NIST)* (2020).
- Nie, L., Kumar, A., Zhan, S., 2014. Periocular recognition using unsupervised convolutional rbm feature learning. *International Conference on Pattern Recognition (ICPR)*, 399–404.
- Nigam, I., Vatsa, M., Singh, R., 2015. Ocular biometrics: A survey of modalities and fusion approaches. *Information Fusion* 26, 1–35.
- Ogawa, K., Kameyama, K., 2021. Adaptive selection of classifiers for person recognition by iris pattern and periocular image, in: Mantoro, T., Lee, M., Ayu, M.A., Wong, K.W., Hidayanto, A.N. (Eds.), *Neural Information Processing*, Springer International Publishing. pp. 656–667.
- Oh, K., Oh, B.S., Toh, K.A., Yau, W.Y., Eng, H.L., 2014. Combining sclera and periocular features for multi-modal identity verification. *Neurocomputing* 128, 185198.
- Opitz, M., Waltner, G., Poier, G., Possegger, H., Bischof, H., 2016. Grid loss: Detecting occluded faces. *European Conference on Computer Vision (ECCV)*, 386–402.
- Padole, C.N., Proena, H., 2012. Periocular recognition: Analysis of performance degradation factors. *International Conference on Biometrics (ICB)*, 439–445.
- Park, U., Jillela, R.R., Ross, A., Jain, A.K., 2011. Periocular biometrics in the visible spectrum. *IEEE Transactions on Information Forensics and Security (TIFS)* 6, 96–106.
- Park, U., Ross, A., Jain, A.K., 2009. Periocular biometrics in the visible spectrum: A feasibility study. *International Conference on Biometrics: Theory, Applications, and Systems (BTAS)*, 1–6.
- Patel, B., Maheshwari, R., Raman, B., 2017. Evaluation of periocular features for kinship verification in the wild. *Computer Vision and Image Understanding (CVIU)* 160, 24–35.
- Pereira, T.d.F., Marcel, S., 2015. Periocular biometrics in mobile environment. *International Conference on Biometrics Theory, Applications and Systems (BTAS)*, 1–7.
- Proena, H., 2014. Ocular biometrics by score-level fusion of disparate experts. *IEEE Transactions on Image Processing (TIP)* (2014) 23.
- Proena, H., Briceo, J.C., 2014. Periocular biometrics: constraining the elastic graph matching algorithm to biologically plausible distortions. *IET Biometrics* 3, 167–175.
- Proena, H., Neves, J.C., 2018. Deep-PRWIS: Periocular recognition without the iris and sclera using deep learning frameworks. *IEEE Transactions on Information Forensics and Security (TIFS)* 13, 888–896.
- Proena, H., Neves, J.C., 2019. A reminiscence of mastermind: Iris/periocular biometrics by in-set CNN iterative analysis. *IEEE Transactions on Information Forensics and Security (TIFS)* 14, 1702–1712.
- Proena, H., Neves, J.C., Santos, G., 2014. Segmenting the periocular region using a hierarchical graphical model fed by texture / shape information and geometrical constraints. *International Joint Conference on Biometrics (IJCB)*, 1–7.
- Qin, B., Li, D., 2020. Identifying facemask-wearing condition using image super-resolution with classification network to prevent COVID-19s. *Sensors* (2020) 20.
- Raghavendra, R., Busch, C., 2016. Learning deeply coupled autoencoders for smartphone based robust periocular verification. *International Conference on Image Processing (ICIP)*, 325–329.
- Raghavendra, R., Raja, K.B., Yang, B., Busch, C., 2013. Combining iris and

- periocular recognition using light field camera. *Asian Conference on Pattern Recognition (ACPR)*, 155–159.
- Raja, K.B., Raghavendra, R., Busch, C., 2014a. Binarized statistical features for improved iris and periocular recognition in visible spectrum. *International Workshop on Biometrics and Forensics (IWBF)*, 1–6.
- Raja, K.B., Raghavendra, R., Busch, C., 2016a. Biometric recognition of surgically altered periocular region: A comprehensive study. *International Conference on Biometrics (ICB)*, 1–6.
- Raja, K.B., Raghavendra, R., Busch, C., 2016b. Collaborative representation of deep sparse filtered features for robust verification of smartphone periocular images. *International Conference on Image Processing (ICIP)*, 330–334.
- Raja, K.B., Raghavendra, R., Busch, C., 2016c. Dynamic scale selected laplacian decomposed frequency response for cross-smartphone periocular verification in visible spectrum. *International Conference on Information Fusion (Fusion)*, 2206–2212.
- Raja, K.B., Raghavendra, R., Busch, C., 2017. Scale-level score fusion of steered pyramid features for cross-spectral periocular verification. *International Conference on Information Fusion (Fusion)*, 1–7.
- Raja, K.B., Raghavendra, R., Busch, C., 2020. Collaborative representation of blur invariant deep sparse features for periocular recognition from smartphones. *Image and Vision Computing (IVC)* 101, 103979.
- Raja, K.B., Raghavendra, R., Stokkenes, M., Busch, C., 2014b. Smartphone authentication system using periocular biometrics. *International Conference of the Biometrics Special Interest Group (BIOSIG)*, 1–8.
- Raja, K.B., Raghavendra, R., Stokkenes, M., Busch, C., 2015a. Fusion of face and periocular information for improved authentication on smartphones. *International Conference on Information Fusion (Fusion)*, 2115–2120.
- Raja, K.B., Raghavendra, R., Stokkenes, M., Busch, C., 2015b. Multi-modal authentication system for smartphones using face, iris and periocular. *International Conference on Biometrics (ICB)*, 143–150.
- Raja, K.B., Raghavendra, R., Vemuri, V.K., Busch, C., 2015. Smartphone based visible iris recognition using deep sparse filtering. *Pattern Recognition Letters (PRL)* 57, 33 – 42.
- Ramaiah, N.P., Kumar, A., 2016. On matching cross-spectral periocular images for accurate biometrics identification. *International Conference on Biometrics Theory, Applications and Systems (BTAS)*, 1–6.
- Rattani, A., Derakhshani, R., 2017. Ocular biometrics in the visible spectrum: A survey. *Image and Vision Computing (IVC)* 59, 1 – 16.
- Rattani, A., Derakhshani, R., 2017. On fine-tuning convolutional neural networks for smartphone based ocular recognition. *International Joint Conference on Biometrics (IJCB)*, 762–767.
- Rattani, A., Derakhshani, R., Saripalle, S.K., Gottemukkula, V., 2016. ICIP 2016 competition on mobile ocular biometric recognition. *International Conference on Image Processing (ICIP)*, 320–324.
- Rattani, A., Reddy, N., Derakhshani, R., 2017. Convolutional neural network for age classification from smart-phone based ocular images. *International Joint Conference on Biometrics (IJCB)*, 756–761.
- Reddy, N., Rattani, A., Derakhshani, R., 2018a. Comparison of deep learning models for biometric-based mobile user authentication. *International Conference on Biometrics Theory, Applications and Systems (BTAS)*, 1–6.
- Reddy, N., Rattani, A., Derakhshani, R., 2018b. OcularNet: Deep patch-based ocular biometric recognition. *International Symposium on Technologies for Homeland Security (HST)*, 1–6.
- Reddy, N., Rattani, A., Derakhshani, R., 2019. Robust subject-invariant feature learning for ocular biometrics in visible spectrum. *International Conference on Biometrics Theory, Applications and Systems (BTAS)*, 1–9.
- Reddy, N., Rattani, A., Derakhshani, R., 2020. Generalizable deep features for ocular biometrics. *Image and Vision Computing (IVC)* 103, 103996.
- Rigas, I., Economou, G., Fotopoulos, S., 2012. Human eye movements as a trait for biometrical identification. *International Conference on Biometrics: Theory, Applications and Systems (BTAS)*, 217–222.
- Ross, A., Banerjee, S., Chen, C., Chowdhury, A., Mirjalili, V., Sharma, R., Swearingen, T., Yadav, S., 2019. Some research problems in biometrics: The future beckons. *International Conference on Biometrics (ICB)*, 1–8.
- Ross, A., Jillela, R., Smereka, J.M., Boddeti, V.N., Kumar, B.V.K.V., Barnard, R., Hu, X., Pauca, P., Plemmons, R., 2012. Matching highly non-ideal ocular images: An information fusion approach. *International Conference on Biometrics (ICB)*, 446–453.
- Sadr, J., Jarudi, I., Sinha, P., 2003. The role of eyebrows in face recognition. *Perception* 32, 285–293.
- Santos, G., Grancho, E., Bernardo, M.V., Fiadeiro, P.T., 2015. Fusing iris and periocular information for cross-sensor recognition. *Pattern Recognition Letters (PRL)* 57, 52 – 59.
- Santos, G., Hoyle, E., 2012. A fusion approach to unconstrained iris recognition. *Pattern Recognition Letters (PRL)* 33, 984 – 990.
- Santos, G., Proena, H., 2013. Periocular biometrics: An emerging technology for unconstrained scenarios. *Workshop on Computational Intelligence in Biometrics and Identity Management (CIBIM)*, 14–21.
- Sequeira, A.F., Chen, L., Ferryman, J., Wild, P., Alonso-Fernandez, F., Bigun, J., Raja, K.B., Raghavendra, R., Busch, C., de Freitas Pereira, T., Marcel, S., Behera, S.S., Gour, M., Kanhangad, V., 2017. Cross-eyed 2017: Cross-spectral iris/periocular recognition competition. *International Joint Conference on Biometrics (IJCB)*, 725–732.
- Sequeira, A.F., Chen, L., Wild, P., Ferryman, J., Alonso-Fernandez, F., Raja, K., Raghavendra, R., Busch, C., Bigun, J., 2016. Cross-eyed - cross-spectral iris/periocular recognition database and competition. *International Conference of the Biometrics Special Interest Group (BIOSIG)*, 1–5.
- Sharma, A., Verma, S., Vatsa, M., Singh, R., 2014. On cross spectral periocular recognition. *International Conference on Image Processing (ICIP)*, 5007–5011.
- Silva, P.H., Luz, E., Zanlorensi, L.A., Menotti, D., Moreira, G., 2018. Multi-modal feature level fusion based on particle swarm optimization with deep transfer learning. *Congress on Evolutionary Computation (CEC)*, 1–8.
- Smereka, J., Kumar, B., 2017. Identifying the best periocular region for biometric recognition, in: Rathgeb, C., Busch, C. (Eds.), *Iris and Periocular Biometric Recognition*, IET.
- Smereka, J.M., Boddeti, V.N., Vijaya Kumar, B.V.K., 2015. Probabilistic deformation models for challenging periocular image verification. *IEEE Transactions on Information Forensics and Security (TIFS)* 10, 1875–1890.
- Smereka, J.M., Kumar, B.V.K.V., 2013. What is a “good” periocular region for recognition? *Conference on Computer Vision and Pattern Recognition Workshops (CVPR-W)*, 117–124.
- Song, L., Gong, D., Li, Z., Liu, C., Liu, W., 2019. Occlusion robust face recognition based on mask learning with pairwise differential siamese network. *International Conference on Computer Vision (ICCV)*, 773–782.
- Stokkenes, M., Ramachandra, R., Raja, K.B., Sigaard, M.K., Busch, C., 2017. Feature level fused templates for multi-biometric system on smartphones. *International Workshop on Biometrics and Forensics (IWBF)*, 1–5.
- Sun, X., Yao, H., Ji, R., Liu, X.M., 2014. Toward statistical modeling of saccadic eye-movement and visual saliency. *IEEE Transactions on Image Processing (TIP)* 23, 4649–4662.
- Tan, C., Kumar, A., 2012. Human identification from at-a-distance images by simultaneously exploiting iris and periocular features. *International Conference on Pattern Recognition (ICPR)*, 553–556.
- Tan, C., Kumar, A., 2013. Towards online iris and periocular recognition under relaxed imaging constraints. *IEEE Transactions on Image Processing (TIP)* 22, 3751–3765.
- Tan, T., Zhang, X., Sun, Z., Zhang, H., 2012. Noisy iris image matching by using multiple cues. *Pattern Recognition Letters (PRL)* 33, 970 – 977.
- Tapia, J.E., Arellano, C., 2019. Soft-biometrics encoding conditional GAN for synthesis of NIR periocular images. *Future Generation Computer Systems* 97, 503 – 511.
- Ud Din, N., Javed, K., Bae, S., Yi, J., 2020. A novel GAN-based network for unmasking of masked face. *IEEE Access* 8, 44276–44287.
- Uzair, M., Mahmood, A., Mian, A., McDonald, C., 2013. Periocular biometric recognition using image sets. *Workshop on Applications of Computer Vision (WACV)*, 246–251.
- Verma, S., Mittal, P., Vatsa, M., Singh, R., 2016. At-a-distance person recognition via combining ocular features. *International Conference on Image Processing (ICIP)*, 3131–3135.
- Vetrekar, N., Raja, K.B., Ramachandra, R., Gad, R., Busch, C., 2018. Multi-spectral imaging for robust ocular biometrics. *International Conference on Biometrics (ICB)*, 195–201.
- VISOB 2.0. <https://sce.umkc.edu/research-sites/cibit/dataset.html>.
- Vyas, R., 2022. Enhanced near-infrared periocular recognition through collaborative rendering of hand crafted and deep features. *Multimedia Tools and Applications (MTA)*, 1573–7721.
- Wang, K., Kumar, A., 2021. Periocular-assisted multi-feature collaboration for dynamic iris recognition. *IEEE Transactions on Information Forensics and Security (TIFS)* 16, 866–879.
- Wang, Z., Wang, G., Huang, B., Xiong, Z., Hong, Q., Wu, H., Yi, P., Jiang, K., Wang, N., Pei, Y., Chen, H., Miao, Y., Huang, Z., Liang, J., 2020. Masked face recognition dataset and application. *arXiv:2003.09093*.

- Woodard, D.L., Pundlik, S., Miller, P., Jillela, R., Ross, A., 2010a. On the fusion of periocular and iris biometrics in non-ideal imagery. *International Conference on Pattern Recognition (ICPR)* , 201–204.
- Woodard, D.L., Pundlik, S.J., Lyle, J.R., Miller, P.E., 2010b. Periocular region appearance cues for biometric identification. *Conference on Computer Vision and Pattern Recognition - Workshops (CVPR-W)* , 162–169.
- Woodard, D.L., Sundararajan, K., Tobias, N., Lyle, J., 2017. Periocular-based soft biometric classification, in: *Iris and Periocular Biometric Recognition*, IET Digital Library. pp. 197–212.
- Xu, J., Cha, M., Heyman, J.L., Venugopalan, S., Abiantun, R., Savvides, M., 2010. Robust local binary pattern feature sets for periocular biometric identification. *International Conference on Biometrics: Theory, Applications and Systems (BTAS)* , 1–8.
- Yin, X., Zhu, Y., Hu, J., 2020. Contactless fingerprint recognition based on global minutia topology and loose genetic algorithm. *IEEE Transactions on Information Forensics and Security (TIFS)* 15, 28–41.
- Zanlorensi, L.A., Laroca, R., Lucio, D.R., Santos, L.R., au2, A.S.B.J., Menotti, D., 2020. Ufpr-periocular: A periocular dataset collected by mobile devices in unconstrained scenarios. *arXiv:2011.12427* .
- Zanlorensi, L.A., Laroca, R., Luz, E., Jr., A.S.B., Oliveira, L.S., Menotti, D., 2021. Ocular recognition databases and competitions: A survey. *Artificial Intelligence Review* 55, 129180.
- Zanlorensi, L.A., Lucio, D.R., d. S. Britto Junior, A., Proena, H., Menotti, D., 2020. Deep representations for cross-spectral ocular biometrics. *IET Biometrics*. 9, 68–77.
- Zhang, M., Zhang, Q., Sun, Z., Zhou, S., Ahmed, N.U., 2016. The BTAS competition on mobile iris recognition. *International Conference on Biometrics Theory, Applications and Systems (BTAS)* , 1–7.
- Zhang, Q., Li, H., Sun, Z., Tan, T., 2018. Deep feature fusion for iris and periocular biometrics on mobile devices. *IEEE Transactions on Information Forensics and Security (TIFS)* 13, 2897–2912.
- Zhao, Z., Kumar, A., 2017. Accurate periocular recognition under less constrained environment using semantics-assisted convolutional neural network. *IEEE Transactions on Information Forensics and Security (TIFS)* 12, 1017–1030.
- Zhao, Z., Kumar, A., 2018. Improving periocular recognition by explicit attention to critical regions in deep neural network. *IEEE Transactions on Information Forensics and Security (TIFS)* 13, 2937–2952.
- Zhou, Z., Du, E.Y., Thomas, N.L., Delp, E.J., 2012. A new human identification method: Sclera recognition. *IEEE Transactions on Systems, Man, and Cybernetics - Part A: Systems and Humans* 42, 571–583.
- Zhu, Z., Huang, G., Deng, J., Ye, Y., Huang, J., Chen, X., Zhu, J., Yang, T., Guo, J., Lu, J., Du, D., Zhou, J., 2021. Masked face recognition challenge: The WebFace260M track report. *arXiv:2108.07189* .